

**On the onset of secondary stability in the wake of two  
rotating cylinders in tandem arrangement**



Author

**Muhammad Aneeb Siddiqui**

Reg No # 356422

Department of Mechanical Engineering  
School of Mechanical and Manufacturing Engineering  
National University of Sciences and Technology  
Islamabad, Pakistan

2024

# **On the onset of secondary stability in the wake of two rotating cylinders in tandem arrangement**

Author

**Muhammad Aneeb Siddiqui**

Reg No # 356422

A thesis submitted to the National University of Sciences and Technology,  
Islamabad,  
in partial fulfillment of the requirements for the degree of  
MS Mechanical Engineering

Supervisor: Dr. Muhammad Nafees Mumtaz Qadri

Co Supervisor: Dr. Adnan Munir

Department of Mechanical Engineering,  
School of Mechanical and Manufacturing Engineering,  
National University of Sciences and Technology,  
Islamabad, Pakistan

2024

## THESIS ACCEPTANCE CERTIFICATE

Certified that final copy of MS Thesis written by Mr       MUHAMMAD ANEEB SIDDIQUI       (Registration No. 356422), of School of Mechanical and Manufacturing Engineering has been vetted by undersigned, found complete in all respects as per NUST Statutes/ Regulations/ Masters Policy, is free of plagiarism, errors, and mistakes and is accepted as partial fulfillment for award of Masters degree. It is further certified that necessary amendments as point out by GEC members and foreign/ local evaluators of the scholar have also been incorporated in the said thesis.

Signature: \_\_\_\_\_



Name of Supervisor Dr M Nafees Mumtaz Qadri


Date: 26<sup>th</sup> September 2024

Signature (HOD): \_\_\_\_\_



Date: 26<sup>th</sup> September 2024

Signature (Dean/ Principal) \_\_\_\_\_



Date: 26<sup>th</sup> September 2024



**National University of Sciences & Technology (NUST)**  
**MASTER'S THESIS WORK**

We hereby recommend that the dissertation prepared under our supervision by: Muhammad aneeb Siddiqui (00000356422)  
Titled: On the onset of secondary stability in the wake of two rotating cylinders in tandem arrangement be accepted in partial fulfillment of the requirements for the award of MS in Mechanical Engineering degree.

**Examination Committee Members**

- |    |                       |  |
|----|-----------------------|--|
| 1. | Name: Asad Javed      | Signature:  |
| 2. | Name: Adnan Munir     | Signature:  |
| 3. | Name: Emad Ud Din     | Signature:  |
| 4. | Name: Saad Ayub Jajja | Signature:  |

**Supervisor:** Muhammad Nafees Mumtaz Qadri

Signature: 

Date: 25 - Sep - 2024



Head of Department

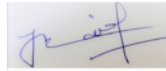
25 - Sep - 2024

Date

**COUNTERSIGNED**

25 - Sep - 2024

Date



Dean/Principal


## CERTIFICATE OF APPROVAL

This is to certify that the research work presented in this thesis, entitled “On the onset of secondary stability in the wake of two rotating cylinder in tandem arrangement” was conducted by Mr. MUHAMMAD ANEEB SIDDIQUI under the supervision of Dr. Muhammad Nafees Mumtaz Qadri.

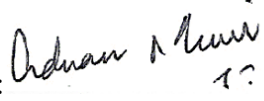
No part of this thesis has been submitted anywhere else for any other degree. This thesis is submitted to the School of Mechanical and Manufacturing Engineering, National University of Sciences and Technology in partial fulfillment of the requirements for the degree of Master of Science in Field of Mechanical Engineering.

Department of Mechanical Engineering, SMME, National University of Sciences and Technology, Islamabad.

Student Name: M Aneeb Siddiqui

Signature: 

a) Dr Adnan Munir (Co-Supervisor)  
Assistant Professor, ME Dept, SMME, NUST

Signature: 

b) Dr Emad-ud-din  
Professor, ME Dept, SMME, NUST

Signature: 

c) Dr Asad Javed  
Assistant Professor, ME, SMME, NUST

Signature: 

d) Dr Saad Ayub Jajja  
Assistant Professor, ME, SMME, NUST

Signature: 

Supervisor Name: Dr Muhammad Nafees Mumtaz Qadri

Signature: 

Name of Dean/HOD: Dr Mian Ashfaq Ali

Signature: 

## **AUTHOR'S DECLARATION**

I, Muhammad Aneeb Siddiqui, certify that this research work titled “On the onset of secondary stability in the wake of two rotating cylinder in tandem arrangement” is my own work and has not been submitted previously by me for taking any degree from National University of Sciences and Technology, Islamabad or anywhere else in the country/world.

At any time if my statement is found to be incorrect even after I graduate, the university has the right to withdraw my MS degree.



---

Muhammad Aneeb Siddiqui

Reg No # 356422


Date: 31-07-2024

## **PLAGIARISM UNDERTAKING**

I solemnly declare that research work presented in the thesis titled “**On the onset of secondary stability in the wake of two rotating cylinder in tandem arrangement**” is solely my research work with no significant contribution from any other person. Small contribution/ help wherever taken has been duly acknowledged and that complete thesis has been written by me.

I understand the zero tolerance policy of the HEC and National University of Sciences and Technology (NUST), Islamabad towards plagiarism. Therefore, I as an author of the above titled thesis declare that no portion of my thesis has been plagiarized and any material used as reference is properly referred/cited.

I undertake that if I am found guilty of any formal plagiarism in the above titled thesis even after award of MS degree, the University reserves the rights to withdraw/revoke my MS degree and that HEC and NUST, Islamabad has the right to publish my name on the HEC/University website on which names of students are placed who submitted plagiarized thesis.

Student Signature: 

Name: Muhammad Aneeb Siddiqui

## ACKNOWLEDGEMENTS

I am grateful to my Creator Almighty Allah for enabling me to pursue this research activity and completing it in an appropriate manner. I am nothing but what You allow me to do. Any help or support which I have during this process is all by Your will.

I am indebted to my parents who not only brought me up but also provided me with all the necessities, either physical or spiritual, to get to the point where I currently stand. It's all your sacrifices, unwavering support and prayers which motivated me to continue up to this stage. My academic performance is merely result of your tireless efforts and support.

I am sincerely thankful to my supervisor Dr Muhammad Nafees Mumtaz Qadri for his insightful guidance and constant support during my research timeframe. His patience on my shortcomings and positive feedback on my mistakes proved instrumental in shaping my research ability, eventually taking this research work to considerable conclusion. I am grateful to my co-supervisor Dr. Adnan Munir for his support during all this time. Nothing would have been possible without his support and motivation.

Finally, I would like to thank my brother and sister for backing me up all the time. My friends and lab mates helped me at every step.



## ABSTRACT

Fluid dynamic transport around a body naturally observe unstable flow behind the body including different patterns of vortical shedding. But simultaneous imposition of rotation to vortex shedding bluff body results in flow stabilization. Eventually, steady flow behind a bluff body is obtained by precisely controlling its overall rotation. In this study critical rotational speeds for two circular cylinders in tandem arrangement are focused for the initiation and termination of secondary vortices in an unconfined flow. Also, the effect of altering the cylinders gap ratios and rotation rates over the obtained flow regimes and respective force coefficients is studied in detail.

Two circular cylinders are subjected to a uniform free stream flow of 100 Reynold number ( $\rho U_{\infty} D / \mu$ ) with varying gap ratios of 1.5, 2 and 4 L/D (center to center) each. At each angular rotation ( $\omega D / U_{\infty}$ ) two modes of rotation are observed, firstly when both the cylinders are made to rotate in the same direction (anticlockwise rotation in this study), secondly when upstream cylinder is rotated in anticlockwise direction and downstream cylinder is rotated in clockwise direction, thus capturing all the possible combinations of two tandem rotating cylinders. Non-dimensional angular rotations ( $\alpha$ ) applied to cylinders vary all the way from stationary to the specific  $\alpha$  where the secondary instability subsides.

Multiple flow regimes along with their sub-divisions are outlined for co-rotation and counter-rotation of two circular cylinders in tandem arrangement depending on the vortical shed pattern. For co-rotation transitions in flow regimes are noticed from 0 to  $6\alpha$ . Gap ratios of 1.5 L/D and 2 L/D show Solitary Periodic (SP) flow where vortices shed in a periodic manner at stationary and low  $\alpha$  values. But for a higher gap ratio of 4 L/D, alternate co-shedding (AC) flow is noticed at stationary and low  $\alpha$  values where both the cylinders show distinct vortical shedding. Increasing  $\alpha$  transits the flow into steady flow referred as SS-I flow regime, where shear layers shed from the combined system of cylinders in a constant manner. Further increment in  $\alpha$  results in the transition of flow from SS-I to secondary unstable state i.e. single rotating bluff body (SRB) flow. SRB flow is sub-divided into two categories termed as integrated and segregated SRB flow obtained at low and high gap ratios respectively. Finally supplementary  $\alpha$  causes wrapping of shear layers around the cylinder with overall steady behavior and thus this flow regime is denoted by SS-II flow regime. It is observed that with the

increase of gap ratio the secondary vortices show delayed transition between distinct flow regimes along with delayed starting and ending of secondary vortices.

For counter rotation of tandem circular cylinders different gap ratios demonstrate distinct flow regimes. Gap ratio of 1.5 L/D shows only SP and SS-I flow regimes. 2 L/D gap ratio illustrates development of three distinct sub-divisions of fundamental SP, SS-I, SRB, and SS-II flow regimes represented as steady state I & II (SS-I & II), secondary unstable - inverted rotation (SU-IR), and secondary unstable (SU-SS-II). Where the upstream and downstream cylinders show dissimilar shedding of vortices or shear layers. Moreover, the transition of these flow regimes from one to another is noticed to be at immensely higher  $\alpha$  values. 4 L/D gap ratio demonstrates generic development of AC, SS-I, SRB and SS-II flow regimes. Except for the 2 L/D case, simulations of various gap ratios for counter-rotating cylinders demonstrate that the  $\alpha$  range extends up to  $6.25\alpha$  for the complete development of all flow states. Flow transitions at atypically higher values of  $12\alpha$  are obtained for gap ratio of 2 L/D.

Force coefficients for both co-rotation and counter-rotation of cylinder show an increase in magnitude with increase of applied  $\alpha$ . Co-rotating and counter-rotating, tandem cylinders show repelling and attractive nature towards each other owing to the rotation derived presence and absence of stagnation point between both the cylinders respectively. Presence of vortex shedding pattern in the force plots is traced using standard deviation of force coefficient ( $\sigma_{CL}$  and  $\sigma_{CD}$ ) plots with reference to the mean force coefficient values. In comparison to the co-rotating cylinder, counter-rotation shows predominant inclination towards stable flow behavior.

Keywords: vortex shedding, tandem cylinders, rotating circular cylinders, vortex suppression

# TABLE OF CONTENTS

<b>ACKNOWLEDGEMENTS</b>	<b>VIII</b>
<b>ABSTRACT</b>	<b>IX</b>
<b>TABLE OF CONTENTS</b>	<b>XI</b>
<b>LIST OF FIGURES</b>	<b>XIII</b>
<b>LIST OF TABLES</b>	<b>XVI</b>
<b>LIST OF ABBREVIATIONS</b>	<b>XVII</b>
<b>CHAPTER 1: INTRODUCTION</b>	<b>1</b>
<b>1.1 Background</b>	<b>1</b>
<b>1.2 Literature review</b>	<b>2</b>
<b>CHAPTER 2: NUMERICAL MODEL AND VALIDATION</b>	<b>9</b>
<b>2.1 Governing equations</b>	<b>11</b>
<b>2.2 Boundary conditions and solver settings</b>	<b>11</b>
<b>2.3 Mesh dependency study</b>	<b>12</b>
<b>2.4 Validation for the computational setup</b>	<b>13</b>
<b>CHAPTER 3: FLOW REGIMES CLASSIFICATION</b>	<b>16</b>
<b>3.1 Co-rotating cylinders</b>	<b>16</b>
3.1.1 Solitary Periodic flow (SP)	17
3.1.2 Alternate Co-shedding flow (AC)	18
3.1.3 Steady State Flow (SS-I)	19
3.1.4 Secondary unstable - single rotating bluff body flow (SU-SRB)	22
3.1.5 Secondary Stable flow (SS-II)	25
<b>3.2 Counter rotating cylinders</b>	<b>26</b>
3.2.1 Solitary periodic flow	27
3.2.2 Alternate co-shedding flow	28
3.2.3 Steady state flow (SS-I)	28
3.2.4 Steady - wrapped combined flow (SS-I&II)	30
3.2.5 Secondary Unstable flow	31
3.2.6 Secondary stable flow (SS - II)	33
<b>CHAPTER 4: STAGNATION POINTS</b>	<b>34</b>
<b>4.1 Gap ratio 1.5 L/D</b>	<b>34</b>
<b>4.2 Gap ratio 2 L/D</b>	<b>36</b>
<b>4.3 Gap ratio 4 L/D</b>	<b>37</b>
<b>CHAPTER 5: LIFT AND DRAG COEFFICIENTS VARIATION AT 100 REYNOLDS NUMBER FOR VARYING ALPHA AND L/D</b>	<b>40</b>
<b>5.1 Force coefficients for co-rotation</b>	<b>40</b>

5.1.1 Gap ratio 1.5 L/D	40
5.1.2 Gap ratio 2 L/D	42
5.1.3 Gap ratio 4 L/D	44
<b>5.2 Force coefficients for counter rotation</b>	<b>47</b>
5.2.1 Gap ratio 1.5 L/D	47
5.2.2 Gap ratio 2 L/D	49
5.2.3 Gap ratio 4 L/D	51
<b>5.3 Results regarding Strouhal Number</b>	<b>52</b>
5.3.1 Strouhal Number vs Reynold Number	55
5.3.2 Strouhal number vs Gap Ratio	55
<b>CHAPTER 6: CONCLUSION &amp; FUTURE WORK</b>	<b>56</b>
<b>REFERENCES</b>	<b>59</b>

## LIST OF FIGURES

Figure 2-1 Schematic diagram for computational domain taken where L/D is 1.5, 2 and 4.....	9
Figure 2-2 Complete computational Mesh for 4 L/D case .....	10
Figure 2-3 Computational mesh in the vicinity of cylinders .....	10
Figure 3-1 Solitary periodic flow for $0\alpha$ at adjacent time steps.....	17
Figure 3-2 Solitary Periodic flow (a) Symmetric at $0\alpha$ 100 Reynolds number (b) Asymmetric $0.5\alpha$ 100 ReNo .....	18
Figure 3-3 Alternate co-shedding (In-Phase) for 100 Reynolds number $4L/D$ at $0\alpha$ and adjacent time steps .....	19
Figure 3-4 Time averaged velocity streamlines for 100 Reynolds number cases at $0\alpha$ .....	19
Figure 3-5 Different modes of Steady fluid regime under increasing $\alpha$ (a) $1\alpha$ slightly asymmetric two shear layers (b) $2\alpha$ expanded negative shear layer (c) $3\alpha$ three shear layer wake (d) $4\alpha$ significantly asymmetric two shear layer wake .....	20
Figure 3-6 Steady flow regime, shear layers modification for increasing $\alpha$ at $4 L/D$ 100 Reynolds number(a) $3\alpha$ (b) $4\alpha$ .....	21
Figure 3-7 Streamlines for steady cases: same rotation of cylinders at 100 Reynolds number(a) $1\alpha$ $1.5L/D$ (b) $1\alpha$ $2 L/D$ (c) $3\alpha$ $4 L/D$ (d) $4\alpha$ $1.5L/D$ (e) $4.5\alpha$ $2 L/D$ (f) $5\alpha$ $4 L/D$ ..	21
Figure 3-8 Integrated Single Rotating Bluff Body flow - 100 Reynold number, $1.5 L/D$ at $5\alpha$ .....	23
Figure 3-9 Segregated SRB flow - 100 Reynold number $4 L/D$ at $5.25\alpha$ .....	24
Figure 3-10 Streamline patterns for SRB flow for 100 Reynolds number at (a) $5\alpha$ $1.5L/D$ (b) $5.25\alpha$ $4 L/D$ .....	24
Figure 3-11 Fully wrapped flow around cylinders at high $\alpha$ at 100 Reynold number (a) $5.5\alpha$ $1.5 L/D$ (b) $5.5\alpha$ $2 L/D$ .....	25
Figure 3-12 SS-II flow regime for $4 L/D$ at 100 Reynold number (a) $5.5\alpha$ (b) $6\alpha$ .....	26
Figure 3-13 Vorticity contours time streak of Asymmetric periodic flow for $1.5 L/D$ , opposite rotation $0.5\alpha$ .....	27
Figure 3-14 Vortex shedding time streak for counter rotating AC flow at $1\alpha$ .....	28
Figure 3-15 Vorticity contours for merged and isolated steady flow states for different gap ratios.....	29

Figure 3-16 Vorticity contours representing secondary shear layers for different gap ratios.....	30
Figure 3-17 Vorticity contour for SS-I&II flow regime for 2L/D at $9\alpha$ .....	31
Figure 3-18 Vorticity contours showing SU-IR flow regimes for 4L/D at $5.5\alpha$ .....	32
Figure 3-19 Vorticity contours demonstrating SU-SS-II flow state for 2L/D at $12\alpha$ ..	32
Figure 3-20 Vorticity contours for SS-II flow state at different gap ratios.....	33
Figure 4-1 Tracing of stagnation points (a) $0.5\alpha$ – total 03 stagnation points (b) $1\alpha$ (c) $3\alpha$ (d) $4\alpha$ – merging of two stagnation points (e) $5\alpha$ (f) $6\alpha$ – relative movement of stagnation points away from the cylinders surfaces with increasing $\alpha$ .....	35
Figure 4-2 Stagnation point tracing 100 Reynold number 2 L/D (a) $0.5\alpha$ - 03 stagnation points (b) $3\alpha$ - stagnation points moving closer to each other (c) $4\alpha$ - two stagnation points about to merge (d) $4.625\alpha$ – overall two stagnation points (e) $4.71875\alpha$ – downstream stagnation point moving away from cylinder surface (f) $5\alpha$ saddle point moving away (g) $5.46875\alpha$ (h) $6\alpha$ .....	37
Figure 4-3 Movement of stagnation points 100 Reynold number - 4L/D (a) $0.5\alpha$ (b) $1\alpha$ (c) $4\alpha$ (d) $5\alpha$ (e) $5.25\alpha$ (f) $6\alpha$ .....	39
Figure 5-1 Mean lift and drag coefficients for upstream (Cylinder-1) and downstream (Cylinder-2) at 1.5L/D.....	41
Figure 5-2 Time averaged flow field 2-D streamlines indicating stagnation point for co-rotating cylinders.....	41
Figure 5-3 $C_L$ and $C_D$ $\sigma$ vs $\alpha$ range plot for 1.5 L/D – Upstream cylinder 1, downstream cylinder 2.....	42
Figure 5-4 Mean lift and drag coefficients for upstream (Cylinder-1) and downstream (Cylinder-2) at 2L/D.....	43
Figure 5-5 $C_L$ and $C_D$ standard deviation vs $\alpha$ range plot for 2 L/D – Upstream cylinder 1, downstream cylinder 2.....	44
Figure 5-6 Mean lift and drag coefficients for upstream (Cylinder-1) and downstream (Cylinder-2) at 4L/D.....	45
Figure 7 $C_L$ and $C_D$ standard deviation vs $\alpha$ range plot for 4 L/D – Upstream cylinder 1, downstream cylinder 2.....	46
Figure 5-8 Force coefficients plot for 1.5L/D at different $\alpha$ .....	48
Figure 5-9 Counter-rotating cylinders flow field visualization via 2-D streamline.....	48
Figure 5-10 Counter rotating cylinders $\sigma$ plots of force coefficients from mean position for 1.5L/D.....	49

Figure 5-11 Mean force coefficient for counter rotating cylinders at  $2L/D$  ..... 50  
Figure 5-12  $\sigma$  plots for counter rotating cylinders at  $2L/D$ ..... 51  
Figure 5-13 Mean force coefficient plots for counter rotating cylinders at  $4L/D$  ..... 52  
Figure 5-14 Counter rotating cylinders  $\sigma$  contours of force coefficients for  $4 L/D$  at  
various  $\alpha$ ..... 52

## LIST OF TABLES

Table 2-1 RMS values comparison for 100 Reynold number simulation results at 0 & $6\alpha$ for three different mesh specifications.....	12
Table 2-2 Non-dimensional flow parameters for stationary two cylinders in tandem arrangement at 100 Reynold number (*UC- upstream cylinder, *DC- downstream cylinder) .....	14
Table 2-3 Non-Dimensional flow parameters for stationary two cylinders in tandem arrangement at 200 Reynold number (*UC- upstream cylinder, *DC- downstream cylinder) .....	15
Table 5-1 Force coefficients variation with different L/D at $6\alpha$ .....	46
Table 5-2 Strouhal Numbers respective to different gap ratios (L/D), angular rotations $\alpha$ and Reynolds Number .....	53



## LIST OF ABBREVIATIONS

$\omega$	Dimensional Rotational Speed
$\alpha$	Non-dimensional Rotation Rate
D	Diameter of Each Cylinder
L	Center-to-center Distance Between Adjacent Cylinders
L/D	Non-dimensional Gap Ratio
$U_{\infty}$	Free-stream Flow Velocity
$\rho$	Density of the Fluid
$\mu$	Dynamic Viscosity of the Fluid
Re	Reynolds Number
$F_L$	Lift Force
$F_D$	Drag Force
$C_L$	Lift Coefficient
$C_D$	Drag Coefficient
$\sigma(C_L)$	Standard Deviation of Lift Coefficients
$\sigma(C_D)$	Standard Deviation of Drag Coefficients
f	Vortex Shedding Frequency
St	Strouhal Number
FFT	Fast Fourier Transform
SB	Single Bluff Body

# CHAPTER 1: INTRODUCTION

## 1.1 Background

Flow around the bluff bodies is marked with different patterns of vortices shedding in the wake. Study of flow around bluff bodies, specifically cylinders has been of paramount importance as it not only provides the clarity about different flow properties but also forms bases for flow field studies around complex geometries. The shedding of vortices induces instability in the flow eventually resulting in application of forces on bluff bodies in directions transverse to the flow. These forces are of great interest in engineering applications as they can cause structural failure owing to resonance and promote multiple fluid phenomenon including noise sources, instability etc. Investigation of these flow derived forces is necessary for designs of offshore structures, heat exchangers or numerous other engineering appliances. There are multiple other applications of flow field study around bluff bodies, for oil exploration purposes the riser bundles linking the offshore platforms with seabed experience shear and oscillatory flows depending upon the waves pattern. In such complex flows the vortex dynamics study carries crucial importance. Control of these vortex induced vibrations is of primary importance from an engineering point of view. Application of rotation to these bluff bodies proposes to be a very promising active flow control method. Rotation of bluff body results in entirely different fluid flow behavior. Moreover, the application of rotation to multiple bluff bodies which are near each other further impacts the flow field. The resultant flow field is influenced by the rotation rate and mutual distance between bluff bodies.

Vortices shedding from bluff bodies can be controlled in several ways. Important considerations include thermal non-homogeneity between the bluff body and fluid passing across it. Wakes of bluff bodies are quite complex as they include the combination of three different shear layers i.e., the boundary layers, separating free shear layer and the wake. And to optimize the wake behind a bluff body several control parameters have been studied, some include.

- Creating thermal non-homogeneity between the moving fluid and the bluff body.
- Use of nanofluids
- Use of control cylinders

- Use of a small cylinder in the vicinity of a cylinder (control rod phenomena)
- Rotation of cylinder / cylinders

## 1.2 Literature review

While performing the earlier fundamental studies for flow around bluff bodies at constant Reynold number, it was noticed that introduction of more than one bluff bodies in the fluid flow causes the relative vortical structures and resulting fluid forces acting of the bluff bodies are completely different in comparison to a single bluff body [1], [2]. Vortex shedding across a bluff body generically initiates in the form of Von Karman vortices when the range of Reynolds number exceed its critical threshold value of 45-50 [3]. This critical Reynolds number differs depending upon the geometrical arrangement of bluff bodies and the properties of operating fluid media. The vortical structures behind the bluff body result in different patterns and then dissipate, meanwhile creating a situation of spatial-temporal disturbance in the flow.

Multiple experimental studies on different arrangements of circular cylinders are done by various authors including M. M. Zdravikovich [1] [4], J. R. Meneghini [2], M. Kiya et al [5], [6] etc. All these studies are aimed to better comprehend the fluid flow around different arrangements of bluff bodies. In 1985 Williamson worked on both the side by side and tandem arrangement of circular cylinders and noticed that for a system of circular cylinders, when the two cylinders were placed in side by side configuration with gap ratio less than 2.2 then only one wake is formed and this wake is deflected in the direction of one cylinder, Williamson name this phenomenon as flip-flopping or flopping [7]. It is also observed that for two cylinders in side-by-side arrangement, when the shed vortices are anti-phase to each other then the vortices retained themselves in the overall wake upto larger extent comparative to the in-phase scenario. Then the binary streak of vortices in anti-phase manner is more stable then the in-phase manner. It is reasoned as for the case of in-phase binary vortical shedding both the vortices superimpose to generate a larger single vortex and thus breaking the overall wake from system of cylinders [7].

In the study of fluctuating and time averaged fluid forces acting on a system of two tandem circular cylinders M. Moriya et al [8] observed that the fluctuating lift and drag forces acting on the downstream cylinder were larger than the upstream cylinder. It was also noticed that just before the critical spacing between the cylinders the gap ratio between the tandem

cylinders was very impactful. Author found clear relation between the fluctuating fluid forces on the downstream cylinder and the reattachment position of the shear layers.

For tandem arrangement of circular cylinders, three flow regimes were defined by M.M Zdravikovich [1]. First when the gap ratio is  $1.2D - 1.8D$  (contingent to a specific Reynold number), in here the separating flow from the upstream cylinder is not captured by the wall of the downstream cylinder and thus due to the separating shear layers from the upstream cylinder only one wake is formed. The second flow regime is when the gap ratio ranges from  $1.2D-1.8D \leq L/D \leq 3.4D-3.8D$ , in this case there is a formation of separation bubble behind the upstream cylinder and the separating shear layers reattached at the downstream cylinder. The wake forming behind the downstream cylinder is influenced by the reattachment of shear layer at the downstream cylinder. The third flow regime is for  $L/D > 4$ . In this scenario two vortices shed, one from each cylinder. This specific wake is known as ‘Binary wake’ as it is formed by the combination of two vortices, one from each cylinder. In the first two flow regimes the drag on the downstream cylinder is less than the drag of the upstream cylinder because of the low-pressure region in between both the cylinders. Even the drag on the downstream cylinder may have a negative value.

An important consideration is that for  $L/D$  of 1.5 and 2 the drag on the downstream cylinder starts from negative value and then advances in the positive direction with the increase in the non-dimensional rotation rate  $\alpha$ . But for  $4 L/D$  it starts from the positive value. This observation was also made by S. Mittal et al in 1997 [9]. Reason for the negative drag of the downstream cylinder is linked with the shear layer shedding from the upstream cylinder and then reattaching the downstream cylinder at the trailing surface thus providing a forward force (negative drag) to the downstream cylinder as well as stability to the shedding flow. This also shows the achievement of flow stability using appropriate gap ratios and a lot of work has been done on this aspect of fluid cylinder interaction studies. Because of this negative drag value from the second cylinder the overall drag of the complete system is less than the drag of a single cylinder placed in the fluid flow under similar conditions as this tandem system of circular cylinders [9]. It was also noticed that with the change in orientation of cylinders from pure tandem arrangement to slightly oblique configuration the drag of the downstream cylinder as well as the overall system increase.

Study on the secondary instabilities in the flow field associated with the system of two circular cylinders in tandem arrangement is done by B. S. Carmo et al [10]. Gap ratios range

from 1.2 to 10 was investigated for relative influence on wake interference. The author provided a comparison of fluid properties of tandem cylinders with single cylinder. It was noticed that if the gap ratio is less than the specific value of gap ratio for drag inversion, the downstream cylinder induces a stabilizing effect. Whereas when the gap ratio between two cylinders was greater than the drag inversion spacing then the wake transition occurred in the similar manner as for isolated cylinder, and thus the downstream cylinder induced destabilizing impact.

In this research the effect of rotation over the stability of fluid flows around circular cylinders is studied in-detail. It is noticed by several researchers that the application of rotation to cylinders in a fluid flow causes flow stabilization.

Three main benefits of rotation of cylinders are as follows.

- Increase in the lift
- Decrease in drag
- Suppression of oscillations due to vortices

J. F. Jaminet and C.W. Vanatta were among the early scientists who studied the impact of rotation on the vortical shedding pattern of circular cylinders. It was reported that increasing the cylinder rotation rate the local conditions necessary to generate the vortices weaken by gradually increasing the vortex shedding frequency [11]. The prominent role of flow Reynolds number is also reported in their study. F. Diaz et al [12] studied the 2 - D turbulent wake behind spinning cylinder. Under rotating cylinder impact the near field showed distinct Karman vortex activity but the Karman activity is noticed to disappear in a relative far-off distance. This gradual transition was also noticed by steady increase in Strouhal number comparative to its conventional value.

Impact of angular rotations on the overall force coefficients response of a single cylinder specifically under laminar flow is also studied by [13]. In this study it is noticed that at higher  $\alpha$  values i.e. above  $5\alpha$ , unsteady periodic flow patterns appear which are characterized by very less velocity in comparison to the primary vortical shedding. The impact of cylinder rotation on the flow field around and the required power is studied by [14], where it is clearly

noticed that with the increase the rotation rate large force coefficients can be seen because of magnus effect but the power required to perform this rotation further increase multifold.

Several authors studied the effect of rotation on bluff bodies specifically the cylinders to control the flow field. Because the knowledge of the stationary tandem system of circular cylinders cannot be extrapolated to the rotating circular cylinders as the involved flow complexities make it impossible to predict the flow nature under influence of rotating cylinders and thus separate analyses are required for rotating cylinders [15]. Important contributions for rotation effects around cylinders are mentioned as follows.

M. R. Rastan et al worked on the flow and heat transfer across two inline cylinders [15] and observed that the increase in Reynold number increases the vortex shedding frequency as well as the heat transfer between the cylinders and fluid field. The direction of rotation of cylinders affects the respective direction of drag forces on both the cylinders. The author divided the overall analysis in a total of 04 fluid flow regimes and concluded that the Nusselt number is more dependent on Reynold number and gap ratio in comparison to rotation rate  $\alpha$ .

D. Chatterjee et al studied the rotation induced flow separation in 2-D around two tandem circular cylinders at low Reynold number [16]. Working was done using a Reynold number of 100 and a non-dimensional rotation rate  $3.0; 0 \leq \alpha \leq 2.75$ . It was spotted that the primary vortex shedding continues up to a specific non-dimensional rotation rate and then the flow turns stable and steady. This rotation rate was named as the critical rotation rate which is observed to be dependent on gap ratio between the cylinders. With the increase in the gap ratio, the critical  $\alpha$  first decreases but at large gap ratios the increase in critical  $\alpha$  value is at a higher rate. With increase in the rotation rate the lift and drag show a monotonic increase and decrease respectively, with drag being more sensitive to rotation rate fluctuations.

M. Darvishyadegari and R. Hassanzadeh studied the heat and fluid flow around two co-rotating cylinders in inline arrangement in a 2-D numerical setup at a Reynold number of 200, gap ratios 1.5, 2 and 3 for non-dimensional rotation rate  $\alpha$  0 to 4 [17]. They observed the positional variation of frontal stagnation point with  $\alpha$  variation. Nusselt number was specifically focused in this study, and it was concluded that there is no significant effect of gap ratio on Nusselt number. At a higher  $\alpha$ , Nusselt number distribution occurs on both cylinders.

B. Dehkordi et al studied the laminar and turbulent flow conditions on a combination of two tandem circular cylinders [18]. Study shows that with the increase in the gap ratio the

flow behavior becomes more unstable and flow properties shift more towards characteristic single cylinder flow. It is observed that at higher Reynold number and gap ratio the amplitude of lift force along with its fluctuations increase and thus system becomes more unstable.

A crucial study was done by N. Hosseini et al in which it was observed the flow states along with their transitions in arrays of tandem cylinders [19]. Using DNS at Reynold number of 200, a total of three bluff bodies are used, first two cylinders and the third one either as cylinder or a flat plate. Focus was kept on the local and global stability and sensitivity analysis. Conclusion showed that the location of third body inside the critical stability transition region triggers a global change. But the position of this critical region was quite specific, not too close to the system and not too far.

Various experimental studies are also done, including the experimental study of R. Duvois and T. Andrienne [20] in which the effect of surface roughness of cylinders on different flow regimes was examined upon varying Reynold number and gap ratio. A range of Reynolds numbers is selected for the study varying all the way from 21000 to 395000. It was noticed that for same flow regime the flow parameters at different Reynold numbers are dependent on the surface roughness. Majorly flow regimes depend on three parameters: the Reynolds number, surface roughness and inlet turbulence intensity.

Numerical analysis using the LES technique was done by A. A. Rosa da Silva [21] in which both tandem and side by side arrangements of cylinders was taken into account using immersed boundary methodology. It showed that presence of multiple cylinders affects the location of stagnation points in front of downstream cylinders. Other than the Reynold number, gap ratio and rotation rate the orientation of cylinders do play a very vital role in shedding vortical pattern. Md. Mahbub Alam did a very influential work [22] where he noticed the effect of gap ratio and phase lag over lift profile and Strouhal number of two tandem cylinders. His study ranges gap ratio from 2 to 9 for a Reynold number of 200. An optimized equation was developed for referencing the relation between lift, gap ratio and phase lag. Respective equation shows that the phase lag is a non-linear function of gap ratio, Strouhal number and convection velocity of the vortices.

Ansari et al [23] studied fluid flow and heat transfer for the co-rotation and counter rotation of two circular cylinders in multiple arrangements at 200 Reynolds number,  $1.5 \leq L/D$

$\leq 4$  and  $0 \leq \alpha \leq 5$ . It was observed that the critical rotation rates for co-rotating cylinders were 20% more than the counter rotating cylinders in different arrangements.

From the literature it is also observed that the flow over co-rotating and counter rotating cylinders differs in terms of generated flow regimes and respective force coefficients [15], [24], [25], [26]. Enhanced flow stability is seen for the flow field with application of counter rotation to a system of two side by side circular cylinders by Yoon et al [24].  $\alpha$  range of 0 to 2 is studied at 100 Reynolds number for 0.2, 0.7, 1.5 and 3 center to center gap ratios. Prominent findings for this study include the tracing of accurate  $\alpha$  at which the primary unstable behavior of two side by side cylinders shift into steady flow state along with mapping of multiple flow regimes observed during this transition. Additional flow regimes are observed for counter rotating cylinders comparing to co-rotating cylinders. But the working was only restricted to side-by-side circular cylinders.

A.S. Chan and A. Jameson also noticed that for counter rotating side by side cylinders, at higher rotational speeds virtual elliptic body is observed to be generated by closed streamlines which strongly resemble a doublet like potential flow [26]. Based on rotation orientation of counter rotating circular cylinders, authors divided the flow into two configurations name as doublet and reverse-doublet. It is reported that in addition to hampering the strength of vortical shedding, complete suppression of unsteady vortex wakes can be achieved by application of counter rotation to circular cylinders. Drag reduction was majorly noticed because of decrease in form drag.

Impact of angular rotation  $\alpha$  for side by side arrangement of two circular cylinders was also studied by S. Kumar et al [11] for different gap ratios and Reynolds numbers. Experimental study using advance flow visualization schemes was done to track down the vortex suppression rotation rate  $\alpha$ . It was noticed that sense of rotation (i.e. inward rotation or outward rotation) play a prominent role in the critical  $\alpha$  value marking vortex suppression. Wake pattern was also observed to shift from in-phase to anti-phase mode respective to applied rotation  $\alpha$ . Focus was kept on tracing the transition from primary unstable to stable state at low angular rotation value.

From all the above studies it was inferred that a vast amount of research has been done on flow across circular cylinders. The effect of rotation of cylinders in tandem and side by side arrangement is also investigated but majority of the work is done on the low angular rotations focusing the primary stability of the overall system.



Whereas the author feels that to fully implement the system of cylinder in practical applications there is need to study all the aspects of fluid flow considering the real-life environment. And thus, this study focuses on the fluid flow response of system of circular cylinders in tandem arrangement under high angular rotation. And as the literature shows the higher angular rotation is linked with the secondary vortical shedding so as the study encapsulates the initiation and termination of secondary vortices, marking the secondary instability. Characteristics of secondary vortices, variation in their strength from starting till vanishing with the variation of  $\alpha$  of cylinders are considered in detail in the present study.

## CHAPTER 2: NUMERICAL MODEL AND VALIDATION

In the present study, 2D flow is considered for numerical simulations. Computational domain considered for the tandem arrangement of circular cylinders in the present study is shown in the Figure 2-1. Gap ratio represented by  $L/D$ , where  $L$  is center to center dimensional distance between tandem cylinders and  $D$  is the diameter of each cylinder, is varied for 1.5, 2 and 4 corresponding to three different cases studied. Rotational speed ( $\omega$ ) applied to each cylinder is normalized using  $\alpha = \omega D/U_\infty$  formulation. Upstream flow velocity is expressed using Reynolds number  $Re = \rho U_\infty D/\mu$  taken as a constant value of 100. Working domains for all the cases is kept larger than the generally used domain in literature. As according to Zhao et al [27] in case of fluid flow study over cylinder if the computational domain is larger than 10 Diameters of the cylinders used as bluff body, then the effect of side boundaries is negligible. But as mentioned by Md Mahbub Alam et al [15] in case of rotating cylinder with rotational speeds greater than  $2\alpha$  (Non dimensional angular rotation) larger domain size is required to keep the shed vortex in reasonable clearance with side boundary. The blockage ratio requirement changes from 5% in stationary cylinders to 1% in rotating cylinder with higher angular velocity. Schematic diagram for the working conditions is represented in the figure below. In the present study the blockage ratio for all the three meshes corresponding to 1.5, 2, 4  $L/D$  is taken as 1.25% to aptly capture the rotations effect on flow field.

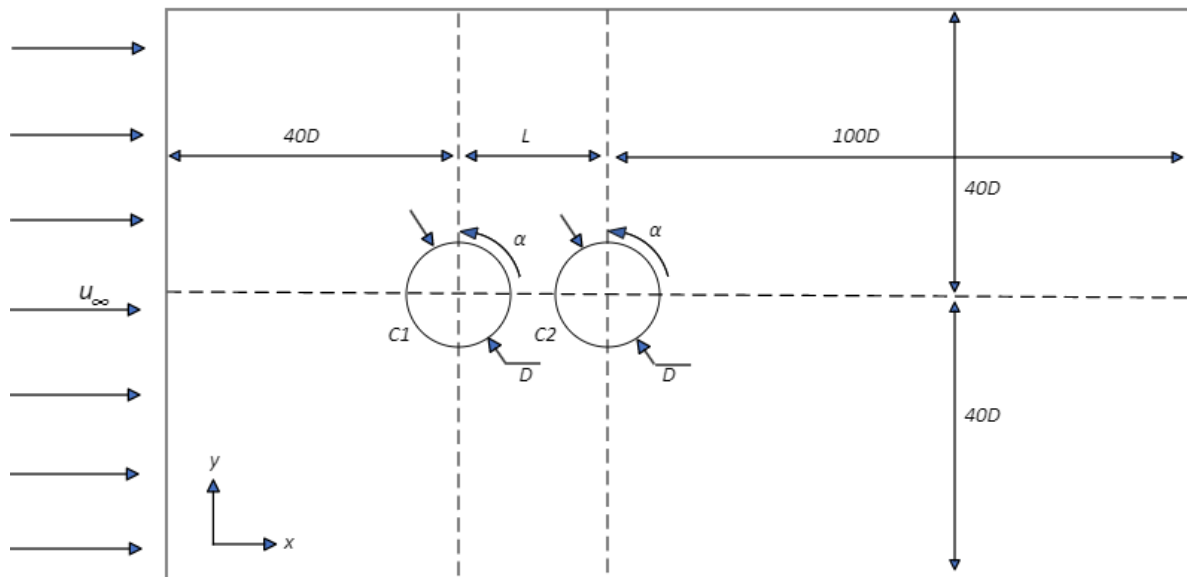


Figure 2-1 Schematic diagram for computational domain taken where  $L/D$  is 1.5, 2 and 4

Analogous to different gap ratios, unique meshes were prepared using ANSYS 18.2. Mesh for 4 L/D gap ratio along with the zoomed mesh near the cylinder surfaces is shown in the figure below.

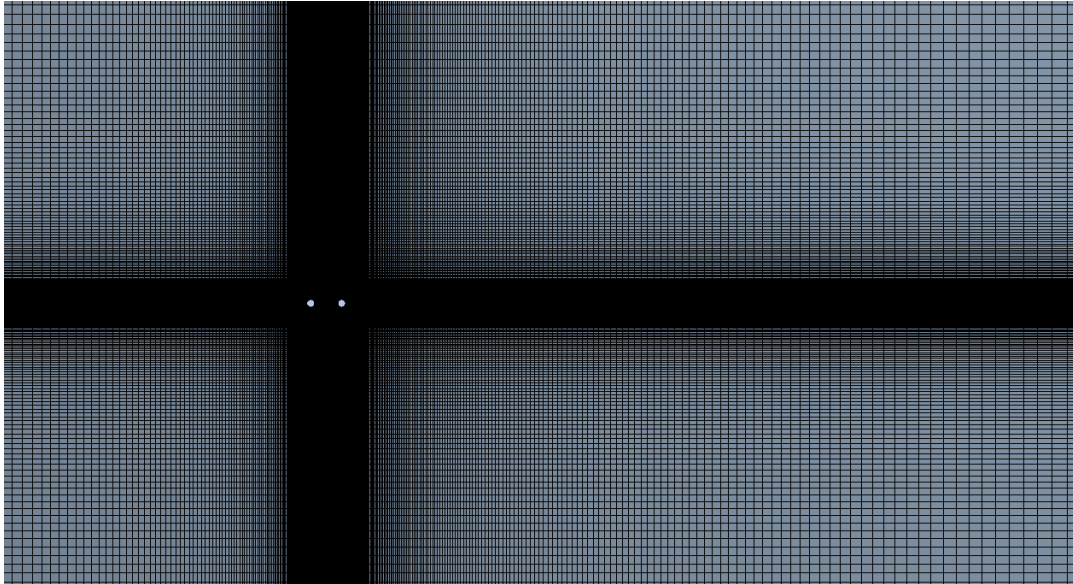


Figure 2-2 Complete computational Mesh for 4 L/D case

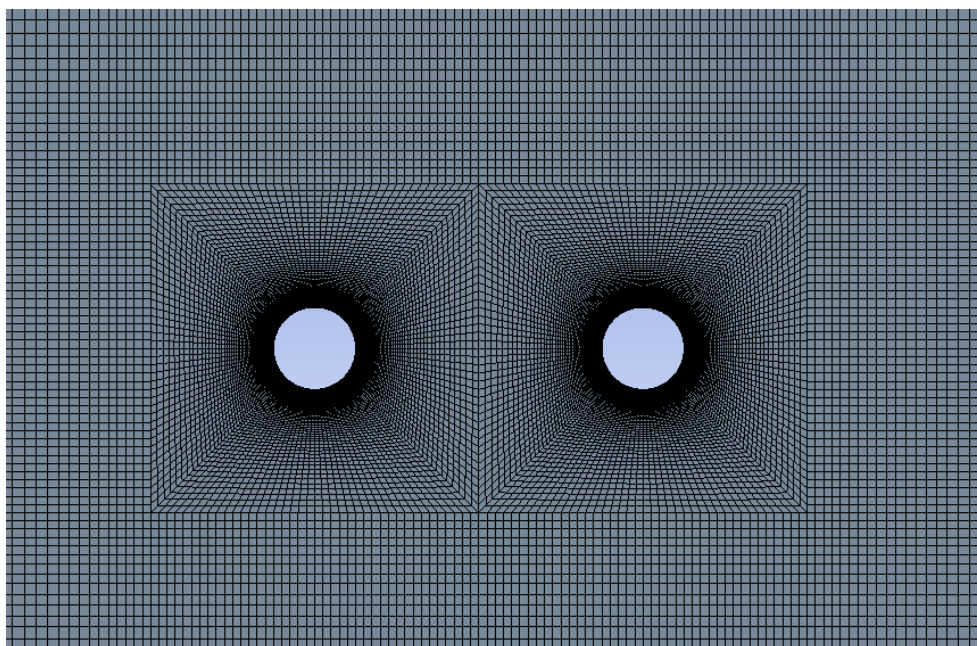


Figure 2-3 Computational mesh in the vicinity of cylinders

Similar meshes are created for 1.5 L/D and 2 L/D. Near the cylinder surfaces the meshes are kept quite dense to capture the shear layer and accurate flow physics in this area.

## 2.1 Governing equations

In this research flow is assumed to be incompressible, viscous and laminar. 2-D Navier Stokes (N-S) equations, taking consideration of streamwise and transverse momentum equations, incompressible continuity are considered. No take part of gravity is assumed for the computational setup. Respective N-S equations in non-dimensional form are expressed as follows.

$$\frac{\partial U}{\partial X} + \frac{\partial V}{\partial Y} = 0 \quad (2.1)$$

$$\frac{\partial U}{\partial T} + U \frac{\partial U}{\partial X} + V \frac{\partial U}{\partial Y} = -\frac{\partial P}{\partial X} + \frac{1}{Re} \left( \frac{\partial^2 U}{\partial X^2} + \frac{\partial^2 U}{\partial Y^2} \right) \quad (2.2)$$

$$\frac{\partial V}{\partial T} + U \frac{\partial V}{\partial X} + V \frac{\partial V}{\partial Y} = -\frac{\partial P}{\partial Y} + \frac{1}{Re} \left( \frac{\partial^2 V}{\partial X^2} + \frac{\partial^2 V}{\partial Y^2} \right) \quad (2.3)$$

Here, the cartesian coordinates  $x$  and  $y$ , time  $t$ , pressure  $p$ , and streamwise and transverse velocities  $u$  and  $v$  are non-dimensionalized as  $X = x/D$ ,  $Y = y/D$ ,  $T = tU_\infty/D$ ,  $P = p/\rho U_\infty^2$ ,  $U = u/U_\infty$  and  $V = v/U_\infty$  respectively

## 2.2 Boundary conditions and solver settings

Boundary conditions for simulations under the N-S equations are defined as follows. Constant velocity is applied in the horizontal direction at the inlet, with streamwise and transverse components as  $u = U_\infty$  and  $v = 0$  respectively. Pressure at the outlet is set to be 0 along with velocity gradients. Symmetric boundary conditions are used for the top and bottom boundaries. Symmetric boundary conditions solve the flow parallel to the boundary using momentum equations whereas no perpendicular flow is considered under this assumption. Non-slip boundary condition is used for the cylinder's surfaces refereeing that the tangential velocity at the cylinder surface is equal to the rotational speed of the cylinder with zero velocity component normal to the surface.

Structured grid of quadrilateral elements is employed for the discretization of N-S equations using finite volume method approach. Pressure velocity coupling is done using Semi-

Implicit Method for Linked Equations (SIMPLE). Second order upwind scheme and central differencing scheme is utilized for the spatial discretization of advection and diffusion terms of N-S equations respectively. Temporal discretization is also done using implicit second order scheme. Non-dimensional time step of 0.001 is used for all the simulations in the present study. Forces acting on each cylinder are sub-divided into lift and drag forces, which are then normalized to lift and drag coefficients using  $C_L = 2F_L/\rho U_\infty^2 D$  and  $C_D = 2F_D/\rho U_\infty^2 D$ . Vortex shedding frequency of the system of cylinders is analyzed using Strouhal Number defined as  $St = fD/U_\infty$ .

### 2.3 Mesh dependency study

In the present study, several meshes are created and studied to capture the most appropriate flow parameters depicting the real-world flows under similar conditions. Each gap ratio study is investigated with 03 different meshes, varying in elemental and nodal densities. And most realistic mesh in the light of literature study and previous studies is opted for further modeling.

To account for the impact of angular rotations on results obtained from different mesh density setups, two analyses states are considered. One stationary and the other  $6\alpha$ , marking the upper threshold for rotation application for majority of the cases. Corresponding results obtained are provided in the Table 2-1.

Table 2-1 RMS values comparison for 100 Reynold number simulation results at 0 &  $6\alpha$  for three different mesh specifications

Gap ratio L/D	Non-dimensional rotation ( $\alpha$ )	Cylinder	60k elements		100k elements		140k elements	
			$C_L$	$C_D$	$C_L$	$C_D$	$C_L$	$C_D$
1.5	0 $\alpha$	UC	0.0110	1.1755	0.0109	1.1759	0.0108	1.1762
		DC	0.0329	0.0850	0.0327	0.0854	0.0324	0.0856
	6 $\alpha$	UC	27.208 4	29.091 2	27.329 8	29.178 7	27.387 6	29.202 3
		DC	28.803	29.891 5	28.933 5	29.986 6	28.996 8	30.015

Gap ratio L/D	Non-dimensional rotation ( $\alpha$ )	Cylinder	50k elements		90k elements		130k elements	
			$C_L$	$C_D$	$C_L$	$C_D$	$C_L$	$C_D$
2	$0\alpha$	UC	0.0037	1.1460	0.0037	1.1450	0.0036	1.1450
		DC	0.0145	0.0852	0.0142	0.0837	0.0143	0.0840
	$6\alpha$	UC	28.740 2	27.610 4	28.770 8	27.705 2	28.877 9	27.705 1
		DC	30.741 2	28.514 3	30.816 4	28.371 6	30.913 2	28.601 5
Gap ratio L/D	Non-dimensional rotation ( $\alpha$ )	Cylinder	50k elements		90k elements		130k elements	
			$C_L$	$C_D$	$C_L$	$C_D$	$C_L$	$C_D$
4	$0\alpha$	UC	0.2941	1.2486	0.2956	1.2507	0.2968	1.2510
		DC	0.9448	0.6933	0.9541	0.7008	0.9575	0.7019
	$6\alpha$	UC	32.192 9	19.156 1	32.510 5	19.531 1	32.565 5	19.569 6
		DC	31.992 2	20.142 7	32.351 9	20.519 7	32.411 2	20.592 7

From the above results the differences between medium and fine mesh density settings are noticed to be very trivial. A similar trend is noticed for all the gap ratios. As  $0\alpha$  and  $6\alpha$  marks the lower and upper threshold for the impact of rotation rate for majority of the cases in the present study. Thus, medium mesh density settings are employed for further numerical study.

## 2.4 Validation for the computational setup

Vast literature study is done to acquire the validation data for the present research. Different researchers have used various parameters to account for the behavior of cylinders system under different flow conditions. In the current study lift and drag coefficients along with Strouhal numbers are used to perform the validation study. Comparison of these non-dimensional flow parameters including the force coefficients and Strouhal number for stationary cylinders at 100 Reynolds number is presented in Table 2-2. As the cylinders high

rotational speed data for different gap ratios was not vastly available thus the comparison is done with the flow parameters at zero rotational speed for different gap ratios i.e. with the stationary data of cylinders in tandem arrangement. Reference data is taken from different research papers as follows, the blank space in the Table 2-2 shows that the respective author have not provided the quantitative data for that specific flow simulation.

Table 2-2 non-dimensional flow parameters for stationary two cylinders in tandem arrangement at 100 Reynold number (\*UC- upstream cylinder, \*DC- downstream cylinder)

Gap Ratio (L/D)	Cylinder	RMS lift and drag coefficient						Strouhal Number	
		Present study		Mahir and Altac		H. Nemati et al [28]		Present study	H. Nemati et al [28]
		C <sub>l</sub>	C <sub>D</sub>	C <sub>l</sub>	C <sub>D</sub>	C <sub>l</sub>	C <sub>D</sub>		
1.5	UC	0.0109	1.1759	-	-	0.01	1.23	0.1329	0.1308
	DC	0.0327	0.0854	-	-	0.01	0.061	0.1329	0.1308
2	UC	0.0037	1.1450	0.0053 (±0.0075)	1.225	-	-	0.1215	-
	DC	0.0142	0.0837	0.0182 (±0.0258)	±0.00012	-	-	0.1215	-
4	UC	0.295	1.2507	0.3380 (±0.478)	1.345	-	-	0.1443	0.147
	DC	0.9541	0.7008	1.0288 (±1.455)	0.764	-	-	0.1443	0.147

To further map the accuracy of the computational setup the same simulations are run at 200 Reynolds number and the corresponding results are compared with the literature available for two tandem cylinders at 200 Reynolds number.

Table 2-3 shows the comparison of force coefficients and the Strouhal number data at 100 Reynolds number for present study and prior literature. Decent agreement between the results of present study and prior literature shows the appropriate nature of computational setup. And thus, the similar case setups are used to perform further numerical study.

Table 2-3 non-dimensional flow parameters for stationary two cylinders in tandem arrangement at 200 Reynold number (\*UC- upstream cylinder, \*DC- downstream cylinder)

Gap Ratio (L/D)	Cyl	RMS lift and drag coefficient								Strouhal Number			
		Present study		C <sub>D</sub> from Dehkordi behzad et al [18]		Meneghini et al [2]		Mahir and Altac [29]		Present study	Dehkordi behzad et al (7)	Meneghini et al	Mahir and Altac
		C <sub>L</sub>	C <sub>D</sub>	C <sub>L</sub>	C <sub>D</sub>	C <sub>L</sub>	C <sub>D</sub>	C <sub>L</sub>	C <sub>D</sub>				
1.5	UC	0.0150	1.0597	0.014 ±(0.02)	1.05	-	1.06	-	-	0.167	0.175	0.167	-
	DC	0.0381	0.1920	0.0424 ±(0.06)	-0.15	-	-0.18	-	-	0.167	0.175	0.167	-
2	UC	0.0195	1.0259	0.007 (±0.01)	1.03	-	1.03	0.0240 (±0.034)	1.06	0.1329	0.138	0.130	0.130
	DC	0.0847	0.1998	0.028 (±0.04)	-0.16	-	-0.17	0.12 (±0.17)	-0.21	0.1329	0.138	0.130	0.130
4	UC	0.5165	1.1979	-	1.16	0.75	1.18	0.4950 (±0.70)	1.34	0.1689	0.179	0.174	0.181
	DC	1.0850	0.3699	-	0.52	1.5	0.38	1.2728 (±1.80)	0.558	0.1689	0.179	0.174	0.181



## CHAPTER 3: FLOW REGIMES CLASSIFICATION

The simulations are done at 100 Reynold number and gap ratios ( $L/D$ ) values 1.5, 2 and 4 for a range of angular rotations. The non-dimensional angular rotations  $\alpha$  values starting from stationary ( $0\alpha$ ) ranges up to the value where further increase in angular rotation does not yield any viable flow field. Furthermore, refined simulations at the starting and ending of secondary vortices are also done to accurately capture the regime of secondary instability. Analysis is done for two orientations of angular rotations, first when both the cylinders are made to rotate in same direction (in present study anticlockwise direction) and second when both rotate in opposite directions (in present study first anticlockwise second clockwise) as these combinations cover all the possible flow sequences which a tandem combination of two cylinders may experience. This chapter provides detailed investigation about different flow fields and transition between these flow fields based on the gap ratios and applied angular rotations.

Flow regimes significantly depend on the sense of rotation and thus these flow regimes are defined separately for same and opposite rotations. Different flow field are studied using time histories of vorticity contours and time averaged velocity streamlines.

### 3.1 Co-rotating cylinders

A total of 05 flow regimes are recognized with their sub-categories based on phase difference, which are described as below.

- Solitary periodic flow (SP)
- Alternate co-shedding flow (AC)
- Steady state flow (SS)
- Single bluff body flow / secondary instability (SRB)
- Wrapped flow – Secondary Stable Flow (WF)

### 3.1.1 Solitary Periodic flow (SP)

When both the upstream and downstream cylinders are close to each other only one periodic wake pattern forms behind the downstream cylinder. The shear layers from the upstream cylinder envelope the downstream cylinder and move along forming the wake pattern like a single cylinder. This flow regime is termed as the ‘solitary periodic (SP) vortex flow’, as there is only one vortical pattern behind the downstream cylinder. Figure 3-1 shows the time streak periodic pattern of the vortex shedding in this regime.

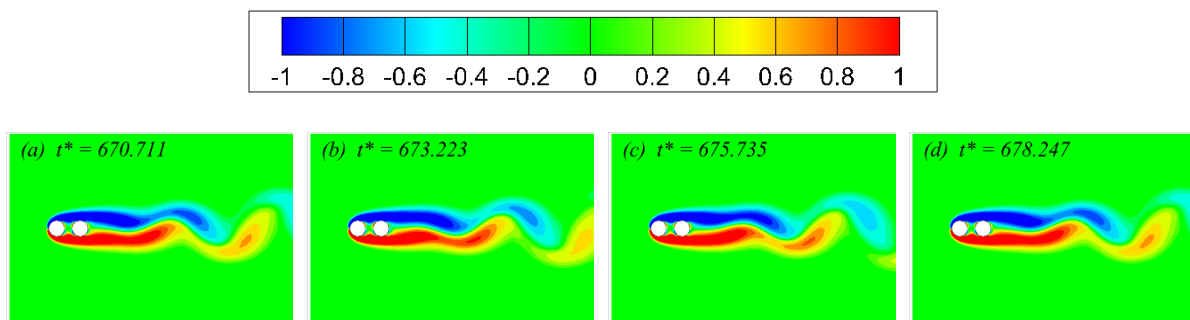


Figure 3-1 Solitary periodic flow for  $0\alpha$  at adjacent time steps

This flow is again subdivided into two categories: the *symmetric solitary periodic flow* and *asymmetric solitary periodic flow* Figure 3-2. When the angular rotation is not applied to any cylinder the periodic flow is symmetric across the horizontal axis but as soon as some angular rotation is applied to any one or both cylinders the vortical shedding shifts to either one side of the horizontal axis thus making the flow as asymmetric periodic flow.

In the current research work this flow regime is observed when simulations are done for  $\alpha$  values of 0 and 0.5 for  $L/D$  range of 1.5 and 2. In literature different authors reported this flow regime as very sensitive to the **gap ratio  $L/D$**  and have quantized this periodic flow regime till gap ratio  $L/D \leq 3.8$ . The same has been observed in the present study but here the effect of non-dimensional angular rotations is also observed in detail.

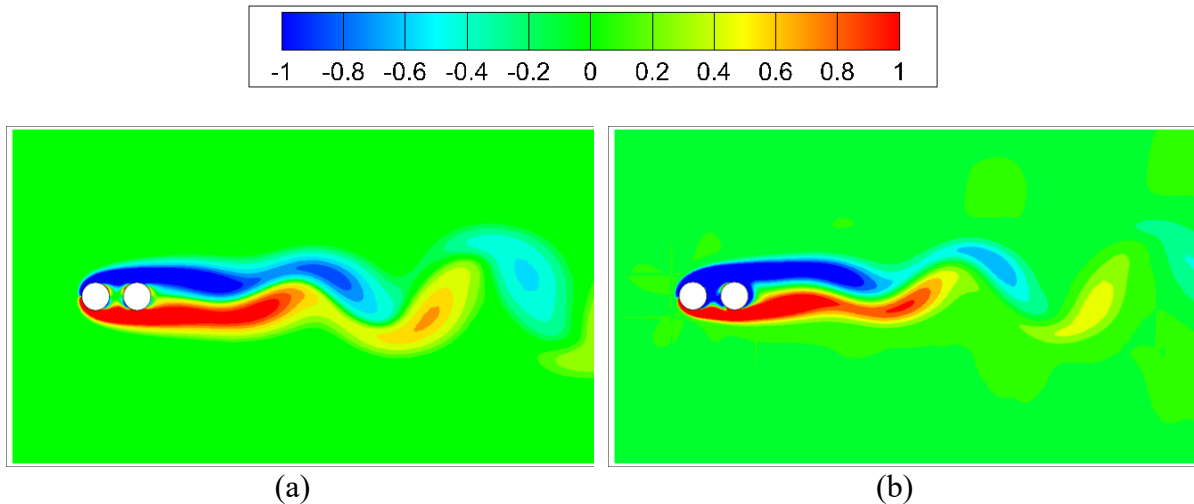


Figure 3-2 Solitary Periodic flow (a) Symmetric at  $0\alpha$  100 Reynolds number (b) Asymmetric  $0.5\alpha$  100 ReNo

### 3.1.2 Alternate Co-shedding flow (AC)

*When the vortices shed from both the upstream and downstream cylinder separately in alternate pattern, this flow condition is referenced as alternating co-shedding AC flow.* It is further observed that there are two types of Alternate Co-shedding flow. M. Md. Alam et al [22] at  $Re = 200$  found the two flow types at  $L/D = 3.65$  and  $5.25$ , respectively.

- When the vortices shedding from the upstream and downstream cylinder are in-phase with each other and thus known as In-phase alternate co-shedding (IAC) flow. Figure 3-3 provides the time history of In-phase alternate co-shedding vortical pattern at  $100ReNo$ ,  $4L/D$  and  $0\alpha$ .
- When the vortices shedding from the upstream and downstream cylinders are not in phase with each other, this flow state is known as Anti-phase alternate co-shedding flow (AAC).

Different authors have observed the transformation of IAC flow to AAC flow with altering gap ratios depending on vortex shedding Strouhal number and vortex convection pattern. Mostly the IAC is observed at gap ratios less than  $5 L/D$  and after that there develops a significant phase lag which ultimately results in AAC. In the current study, IAC flow is observed at  $4 L/D$  at 100 Reynolds number, since this work is limited to  $4 L/D$  hence properly formed AAC flow is not observed.

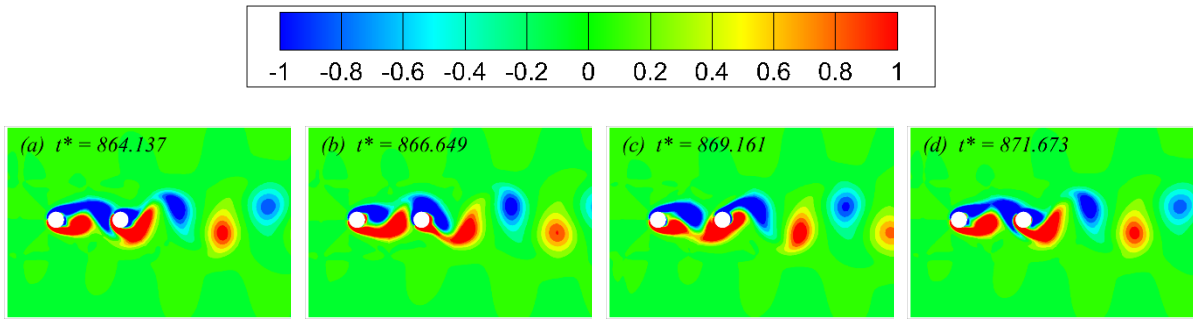


Figure 3-3 Alternate co-shedding (In-Phase) for 100 Reynolds number  $4L/D$  at  $0\alpha$  and adjacent time steps

Flow streamlines for the solitary periodic flow and the alternate co-shedding flow are provided in the Figure 3-4. Averaged velocity streamlines plot provide insight into the flow behavior and the impact of gap ratio between rotating cylinders ultimately highlighting the importance of the arrangement of the cylinders. During this primary unsteady flow regime, the change in gap ratio demonstrates the variation in the vortical patterns forming in between the cylinders as well as in the overall wake of the system. At 1.5 and 2  $L/D$  we notice that the vortical patterns form behind both the upstream and downstream cylinder but as the gap ratio reaches  $4L/D$  the downstream cylinder which is under less influence of the upcoming flow shows less pronounced vortex formation. In this research work AC flow is observed for 4  $L/D$  gap ratio during the  $\alpha$  range of 0 to 2. Whereas this AC flow regime only consists of IAC flow.

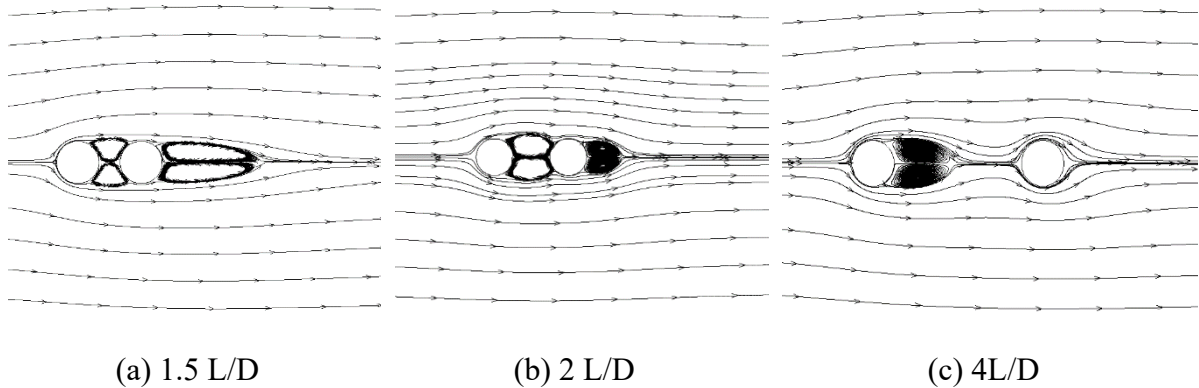


Figure 3-4 Time averaged velocity streamlines for 100 Reynolds number cases at  $0\alpha$

### 3.1.3 Steady State Flow (SS-I)

When flow across the cylinders do not show any dynamic vortex shedding and there is formation of plain shear layers in the wake, or shear layers just wrap around the cylinders, it is referred as the steady state flow.

Steady flow develops with the application of angular rotation  $\alpha$ . For the gap ratio of  $1.5L/D$  and  $2L/D$ , the shear layer facilitated by the angular rotation pushes the counterpart away and thus making the overall wake of the flow asymmetric Figure 3-5 (a). On further increasing the  $\alpha$  the side of cylinder having fluid velocity due to angular rotation, opposite to the upcoming free stream flow experience more expanded shear layer region Figure 3-5 (b). But with significant increase in rotation the negative shear layers shedding from above the downstream cylinder tend to wrap around the downstream cylinder as shown in Figure 3-5 (c). At a little higher alpha, shear layers ultimately arrive at the lower side of wake Figure 3-5 (d). Supplementary  $\alpha$  simply increase the asymmetric behavior of the shedding shear layers with negative shear layer enveloping the cylinders and enforcing the positive shear layer to shed from the upper region of the downstream cylinder Figure 3-5 (d).

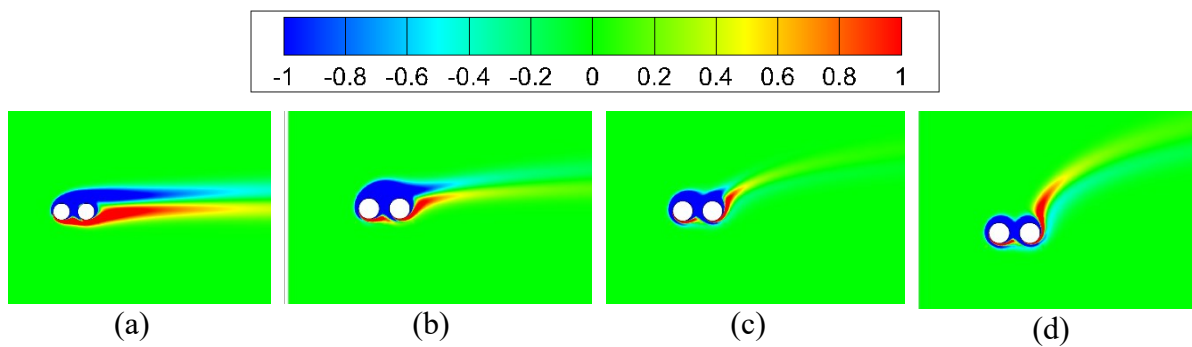


Figure 3-5 Different modes of Steady fluid regime under increasing  $\alpha$  (a)  $1\alpha$  slightly asymmetric two shear layers (b)  $2\alpha$  expanded negative shear layer (c)  $3\alpha$  three shear layer wake (d)  $4\alpha$  significantly asymmetric two shear layer wake

Another steady flow region is observed in case of increased gap ratio, i.e., in present study from  $4L/D$  case. The shear layers from both cylinders do not wrap around each other rather the shear layers from the upstream cylinder fall on downstream cylinder and then a common wake is generated in the form of two or three shear layer patterns. Initially the positive shear layers shed from lower region of the downstream cylinder but eventually with increase in  $\alpha$  the negative shear layers start wrapping around the cylinder, enforcing the positive shear layer to shed from the upper back region of the downstream cylinder Figure 3-6.

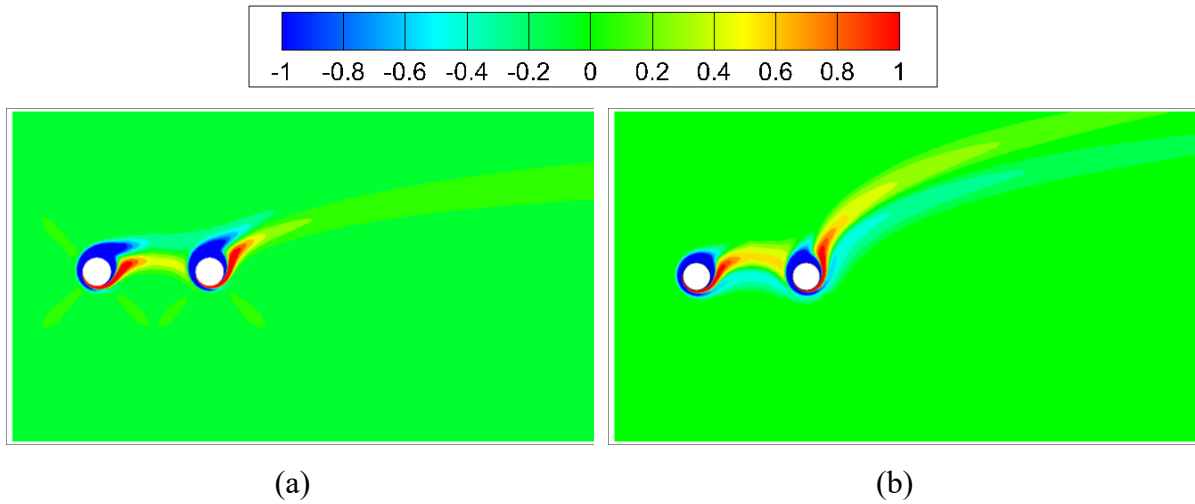


Figure 3-6 Steady flow regime, shear layers modification for increasing  $\alpha$  at 4 L/D 100 Reynolds number (a)  $3\alpha$  (b)  $4\alpha$ .

At 100 Reynold number, SP flow for 1.5 and 2 L/D transition to steady flow at around  $0.5 - 1\alpha$ , continuing up to  $4.5\alpha$ . But for 4 L/D, AC flow transitions to steady flow is in between  $2-3\alpha$  continuing up to  $5\alpha$ . This transition occurs in a smooth and gradual manner, at first the magnitude of vortices from SP and AC flow regimes weakens and the flow becomes steady.

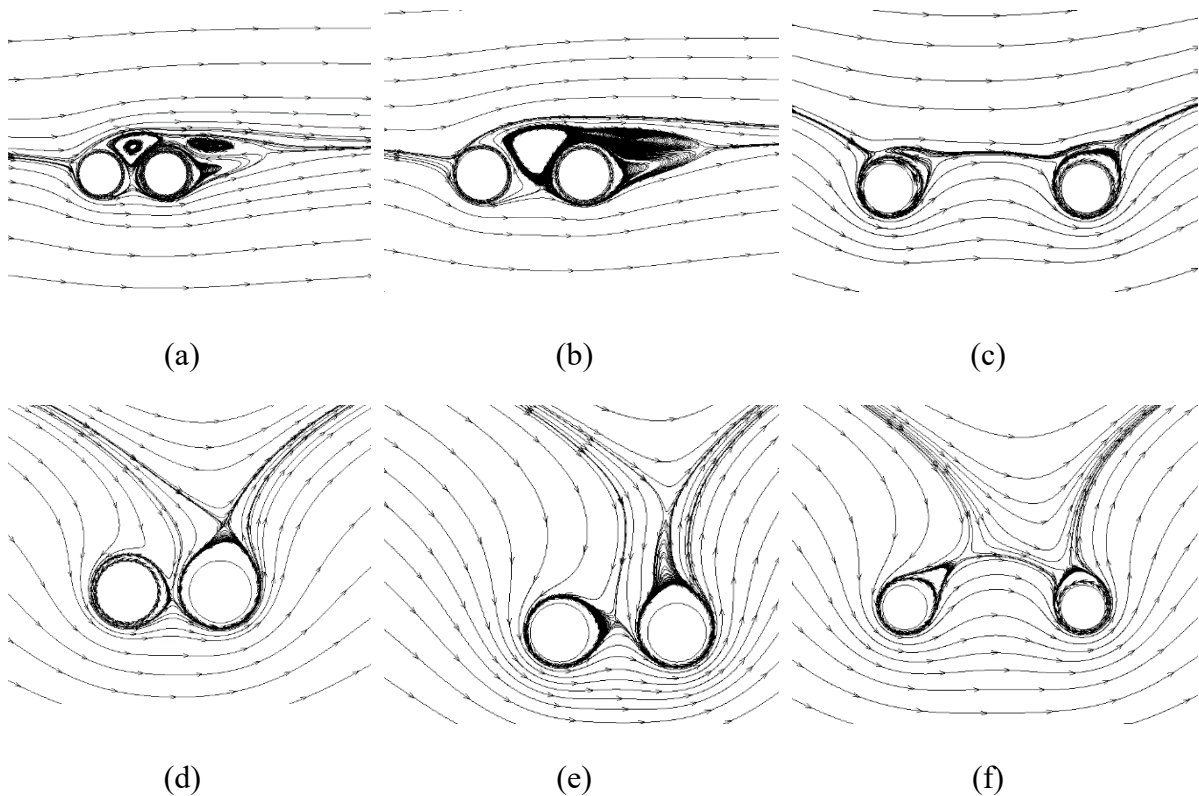


Figure 3-7 Streamlines for steady cases: same rotation of cylinders at 100 Reynolds number (a)  $1\alpha$  1.5L/D (b)  $1\alpha$  2 L/D (c)  $3\alpha$  4 L/D (d)  $4\alpha$  1.5L/D (e)  $4.5\alpha$  2 L/D (f)  $5\alpha$  4 L/D

The effect of gap ratio can also be seen from the above-mentioned transitioning  $\alpha$  ranges. Increased gap ratio delays the transition from unsteady to steady state. It is because at the low gap ratio the shear layers from upstream cylinder easily approach the downstream cylinder whereas for increased gap ratio the shear layers from upstream cylinder do not approach downstream cylinder, resulting in the creation of circulation zones in the gap. The vortices from the upstream cylinder on reaching the downstream cylinder divide in different proportions and appear in the overall wake from both upper and lower sides of downstream cylinder, depending on the provided  $\alpha$ . It causes the flow to be more unsteady, prolonging the AC flow.

Observing the streamline patterns for the steady cases, a very similar fashion is observed, subfigure (a) and (d) Figure 3-7 refers to 1.5 L/D showing the corresponding  $\alpha$  for starting and ending of steady flow regime. Similar fashion is observed for the 2L/D and 4L/D with the exception that at 4L/D both the cylinders behave separately Figure 3-7.

#### *3.1.4 Secondary unstable - single rotating bluff body flow (SU-SRB)*

The vortex shedding pattern at the high angular rotation rate is like the single rotating cylinder flow field at high  $\alpha$ . Thus, this flow regime is named as secondary unstable - single rotating bluff body flow (SU-SRB). In this flow regime the shear layers first wrap around the cylinder then stretch and finally shed downstream as a single strong vortex. This is the secondary unstable flow regime. Current study is specifically focused on this flow state. Accurate mapping of initiation and termination of secondary vortices is done.

Significant differences can be seen in the flow pattern depending upon the gap ratio. And thus, two distinct flow types in SU-SRB flow are defined based on different gap ratios.

##### *3.1.4.1 Integrated SU-SRB flow.*

When the shear layer from upstream cylinder rolls over the downstream cylinder and the overall system of two cylinders shed a larger common vortex from one side of the system instead of the downstream region, it is referred to as the Integrated SU-SRB flow. This flow regime is clearly visible at **lower gap ratios**. Time streak depicting the creation and shedding of the secondary vortex is shown in the Figure 3-8. With increase in  $\alpha$ , the vortex forming above both the cylinders becomes more well defined, the strength of the vortex increases, and

its shedding period elongates. At this stage the force coefficients show an increase in magnitude depicting the strength of vortex forming above the system.

Increasing the gap ratio  $L/D$  delays the SU-SRB flow by hindering the shear layers to stretch across both the cylinders easily.

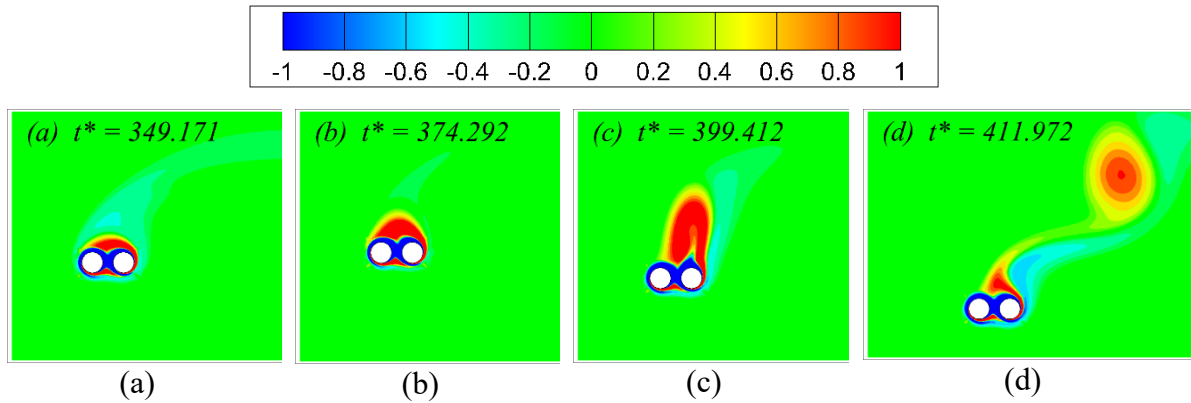


Figure 3-8 Integrated Single Rotating Bluff Body flow - 100 Reynold number, 1.5  $L/D$  at  $5\alpha$

A relation between vortex shedding in SU-SRB flow and in-gap shear layers interference is noticed for small gap ratios. The shear layers keep on wrapping around the cylinder making a positive vortex over both the cylinders, mounting up the region with vorticity. But as soon as the negative shear layer of upstream and downstream cylinder interfere in the gap between both the cylinders the strong vortex mounted above both the cylinder shed in the overall wake of the system. The same process is followed in a repetitive manner.

### 3.1.4.2 Segregated SU-SRB flow

The second type of SU-SRB flow is when the vortex from the upstream cylinder sheds and falls on the downstream cylinder, stretches and then a larger vortex sheds from the downstream cylinder. This is mostly the case when there is enough gap between both cylinders that vortex shedding from the upstream cylinder becomes possible (in present study  $4L/D$ ) as shown in Figure 3-9.

Analysis of flow simulations and force coefficients demonstrate that the alteration in  $\alpha$  and  $L/D$  in this case affects the flow in a similar manner as for integrated SU-SRB flow. A peculiarity observed in this case (100 Reynold number -  $4L/D$ ) is when flow transitioning from steady to SRB flow, wake show oscillatory behavior without formation of complete vortex. It is when the shear layers from the upstream cylinder fall on the downstream cylinder, but the positive shear layers of upstream cylinder interact with the positive shear layer of downstream



cylinder in a continuous manner. And thus, it results oscillations in the wake. A slight increase in  $\alpha$  results in properly developed SU-SRB flow. Force coefficients plots show prominent periodic pattern for this flow state.

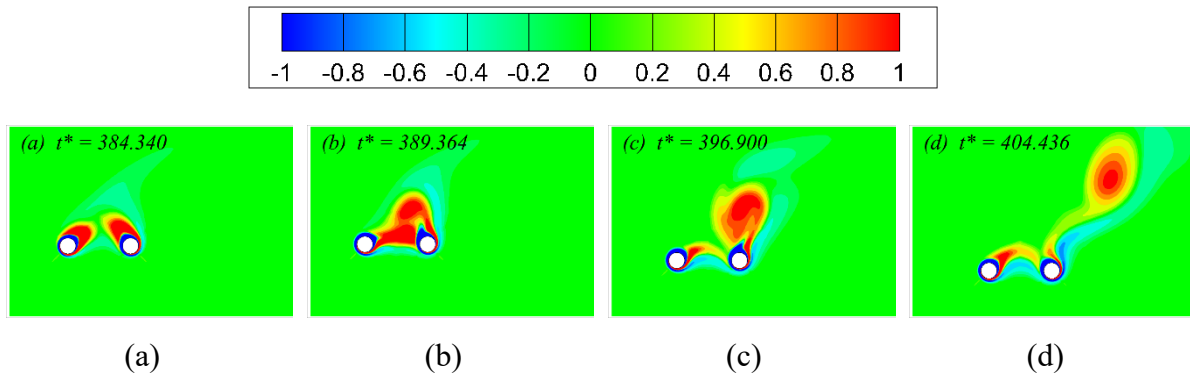


Figure 3-9 Segregated SRB flow - 100 Reynold number 4 L/D at  $5.25\alpha$

For L/D of 1.5 and 2 with the increase in  $\alpha$ , SS-I flow regime transitions to SU-SRB specifically integrated SU-SRB flow at around  $4.5625 - 4.625\alpha$  and  $4.6875 - 4.71875\alpha$  respectively, continuing till  $5.715 - 5.2125\alpha$  and  $5.46875 - 5.5\alpha$  for 1.5 and 2 L/D respectively. Whereas for 4 L/D transition from SS-I to SU-SRB flow state specifically the segregated SU-SRB flow regime occurs at  $5 - 5.0625\alpha$  continuing up to  $5.5625 - 5.625\alpha$  respectively.

From the above-mentioned flow transitioning ranges the effect of gap ratio is observed. With increase in the gap ratio, steady to unsteady transitioning  $\alpha$  delays as vortex from the upstream cylinder first fall on the downstream cylinder and then makes a stronger vortex which sheds in the wake, resulting in overall delay of the transition.

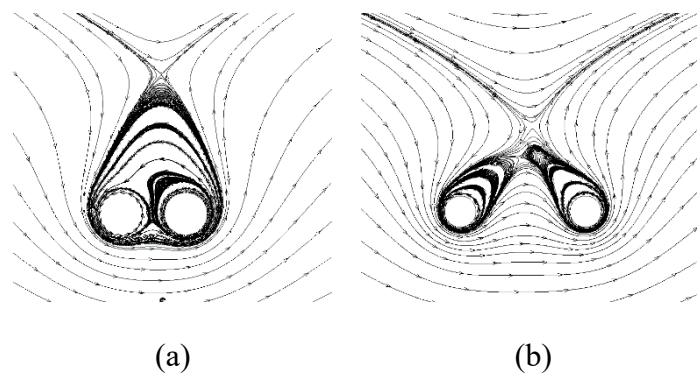


Figure 3-10 Streamline patterns for SRB flow for 100 Reynolds number at (a)  $5\alpha$  1.5L/D (b)  $5.25\alpha$  4 L/D

Considering the streamlines pattern for the integrated and segregated fully developed SU-SRB flows, shown in Figure 3-10, it can be clearly noticed that for integrated SRB flow only one large shear layers enveloping region is formed covering both the upstream and downstream cylinder simultaneously whereas for the segregated SRB flow, both the cylinder make their own envelope of shear layers.

### 3.1.5 Secondary Stable flow (SS-II)

When rotation increase to the extent that the shear layers completely wrap around the cylinders, it is referred as the secondary steady flow regime i.e. SS-II. For lower gap ratios the shear layers envelope both the cylinders collectively. The negative shear layer is enveloped by the positive shear layer which then creates an overall extended vortical region above both the cylinders. With further increase in  $\alpha$  the shear layers budge closer to the cylinder surfaces Figure 3-11 (a) and (b).

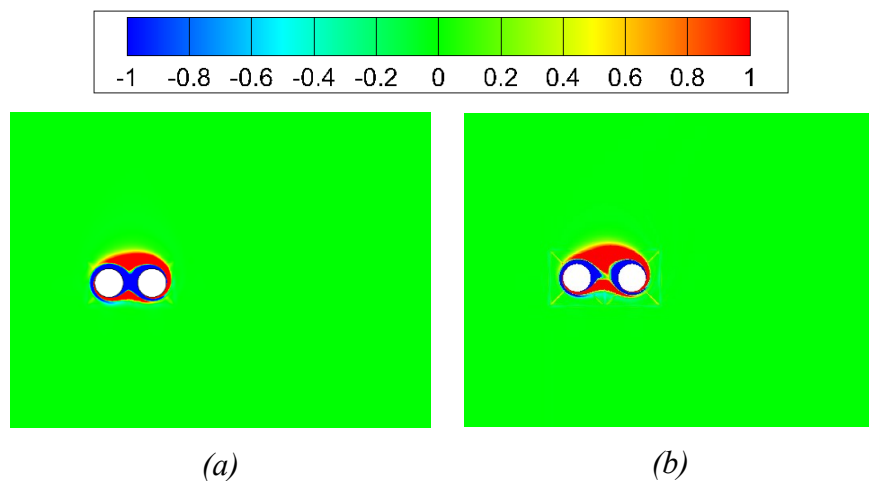


Figure 3-11 Fully wrapped flow around cylinders at high  $\alpha$  at 100 Reynold number (a)  $5.5\alpha$  1.5 L/D  
(b)  $5.5\alpha$  2 L/D

For 4 L/D the flow wraps around both the cylinders separately, with a positive shear layer enveloping the negative one. Extended vortical regions of positive shear layers from both the cylinders are stretched towards the upper center in the gap ratio owing to direction of  $\alpha$  Figure 3-12 (a). Increasing  $\alpha$  causes the shear layers to further move closer to cylinder surfaces Figure 3-12 (b).

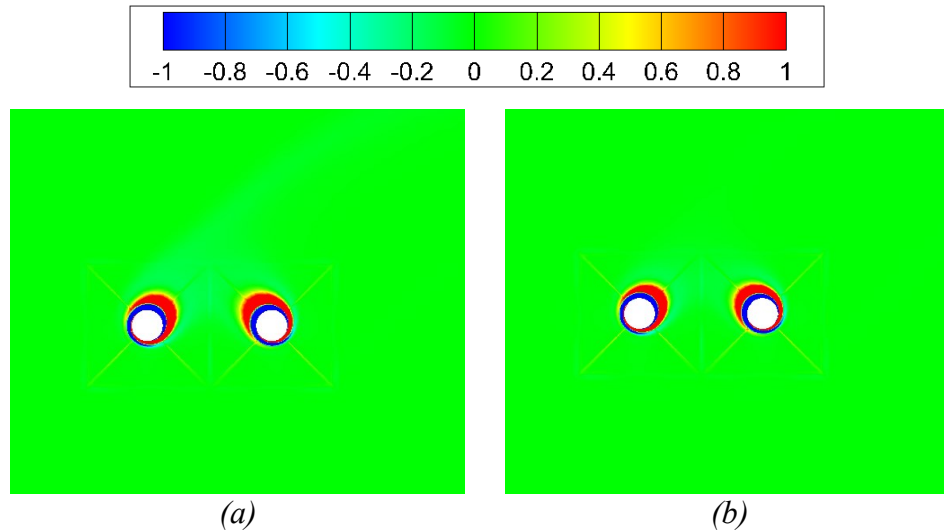


Figure 3-12 SS-II flow regime for 4 L/D at 100 Reynolds number (a)  $5.5\alpha$  (b)  $6\alpha$

Transition from SU- SRB flow to SS-II occurs in a **sudden manner**, unlikely the initiation of SU-SRB regime. During the instigation phase, the SS-I flow gradually shifts to SU-SRB flow with force coefficients progressively mounting up and the time history of force coefficients coming in well-defined periodic pattern (as discussed in the force coefficients Chapter 5). But during the termination of secondary vortices at high  $\alpha$ , there is an abrupt transferal of force coefficients periodic time trace from well-defined periodic wave form to straight line upon slight  $\alpha$  increase. This shows the unstable nature of the SU-SRB flow regime. At 1.5, 2 L/D this transition range from SU-SRB flow to SS-II flow regime is  $5.175 - 5.2125\alpha$  and  $5.46875 - 5.5\alpha$  respectively, whereas for 4 L/D this transition range is  $5.5625 - 5.625\alpha$ .

### 3.2 Counter rotating cylinders

In the present study both the cylinders are also made to rotate in opposite orientation i.e., the first cylinder rotating in anticlockwise direction and the second cylinder rotating in clockwise direction. Overall flow regimes and their transition upon alteration in  $\alpha$  is nearly same as that for the same orientation angular rotation with some complex flow regimes seen during transition from one phase to other.

Total flow regimes observed during application of rotations in opposite orientations are listed as below.

- Solitary periodic flow (SP)
- Alternate co-shedding flow (AC)
- Steady flow (Combined and Segregated Steady Flow)

- Steady - wrapped combined flow (SS-I&II)
- Secondary unstable flow
- Secondary Unstable – Wrapped flow
- Fully wrapped flow

### 3.2.1 Solitary periodic flow

Same as for co-rotating cylinders, the initial unsteady flow state under stationary and low  $\alpha$  values is termed as solitary periodic flow state (SP). At first with the application of slight  $\alpha$  the flow maintains the asymmetric periodic nature but the overall magnitude of periodic vortices in comparison to  $0\alpha$  reduces. It shows ability of angular rotation to shift the flow from periodic vortex shedding to steady flow i.e. unsteady to steady flow state. Figure 3-13 shows the time variation of vorticity contours for  $0.5\alpha$  at four different instances.

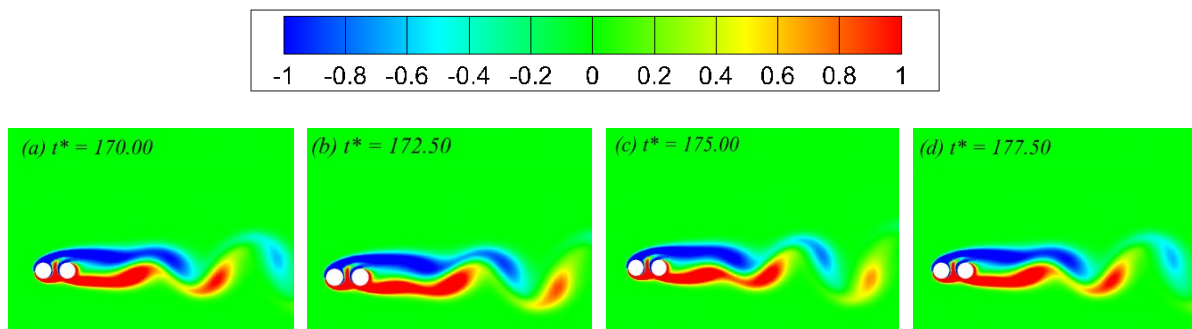


Figure 3-13 Vorticity contours time streak of Asymmetric periodic flow for 1.5 L/D, opposite rotation  $0.5\alpha$

In comparison to the Figure 3-1 showing time variation of tandem cylinders at  $0\alpha$ , in Figure 3-13 positive shear layer from the lower region of the upstream cylinder can be seen advancing upward in the middle region of both cylinders under the influence of downstream cylinder clockwise rotation. This interaction of positive shear layer of upstream cylinder with the negative shear layer of downstream cylinder, traveling from in between both the cylinders induce stability in the overall system and ***thus counter rotating cylinders system achieves early steady state in comparison to the co-rotating cylinder system***. In case of co-rotating cylinders PS regime transits into SS-I in between  $0.75 - 1\alpha$ , whereas for counter rotating cylinders this transition occurs in between  $0.5 - 0.75\alpha$ .

### 3.2.2 Alternate co-shedding flow

For increased gap ratio i.e.  $4L/D$  in present study, the wake pattern shows alternate co-shedding of vortices alike the co-rotating cylinders and thus termed as Alternate co-shedding flow (AC). For opposite sense of rotation of both cylinders, in-phase alternate co-shedding is observed for  $0.5$  and  $1\alpha$ .

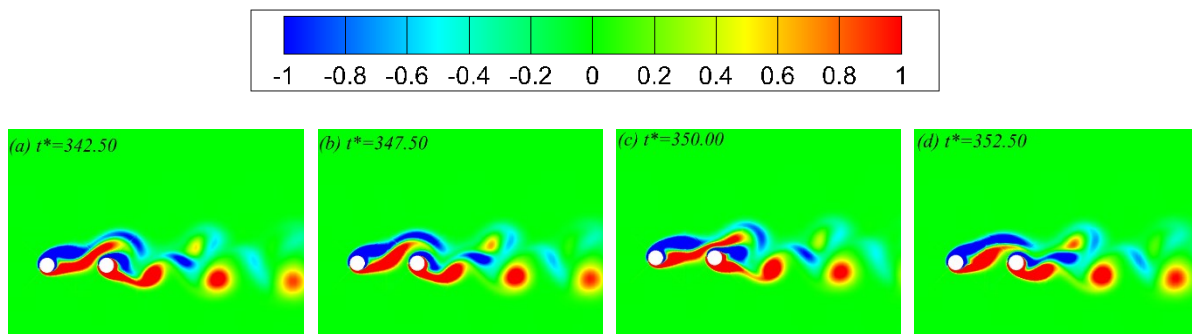


Figure 3-14 Vortex shedding time streak for counter rotating AC flow at  $1\alpha$

Isolated shedding of vortices from both the cylinders can be noticed. Wake of upstream and downstream cylinder translates in the relative directions under the influence of cylindrical rotations. By further increasing the  $\alpha$  the wake from upstream cylinder translates further in the rotation direction, thus making its separate way to the overall wake of the system without making any interaction with the downstream wake.

### 3.2.3 Steady state flow (SS-I)

Transition from the solitary periodic flow and alternate co-shedding flow for  $1.5 - 2L/D$  and  $4L/D$  to steady flow occurs in between ranges of  $0.5-1\alpha$  and  $1 - 2\alpha$  respectively.

In comparison to the steady flow of co-rotating cylinder here two types of steady asymmetric flows are seen depending upon the extent of rotation applied to the cylinders. Initially after the conversion of periodic flow into steady flow with increased rotation, the shear layers from both cylinders merge and then form a combined wake with overall two shear layers of the whole system. But with further enhancement of angular rotation to cylinders, unlike co-rotating cylinders system, wakes of both the cylinders **remain isolated without merging with each other**. Wake of upstream cylinder under the influence of cylindrical rotation goes above the downstream cylinder without any significant interaction. This outcome is observed to augment with the increase in gap ratio. In this flow, the final wake of the system consists of four shear layers. For  $1.5$  and  $2 L/D$  this transition from merged steady flow to segregated

steady flow occurs around  $3-4\alpha$  and  $2-3\alpha$  respectively, but for  $4 L/D$  only segregated steady flow consisting of independent wakes from both cylinders is observed. Thus the flow shifts directly from the alternate co-shedding flow to segregated steady flow. Pictorial representation of both types of steady wakes are shown below.

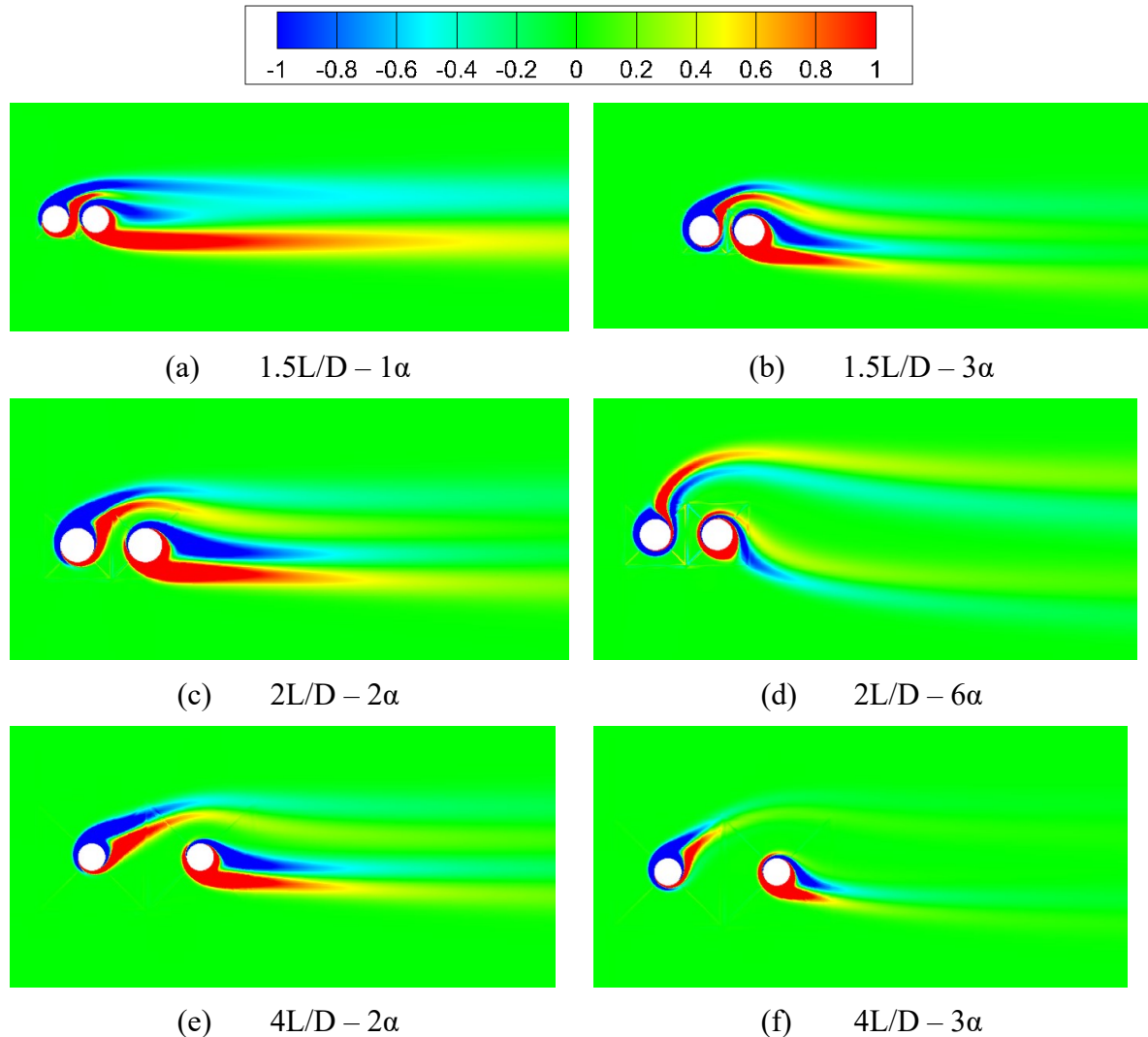


Figure 3-15 Vorticity contours for merged and isolated steady flow states for different gap ratios

With gradual increase in  $\alpha$  values i.e.  $\geq 4.5\alpha$ ,  $4\alpha$  and  $3\alpha$  for  $1.5L/D$ ,  $2L/D$  and  $4L/D$  respectively, it is noticed that the negative shear layer for the upstream cylinder and positive shear layer for the downstream cylinder wrap around the cylinder and join the wake from the opposite side as well enveloping the opposite shear layer. This origination of shear layer from the opposite side is termed as the secondary negative and positive shear layer for the upstream and downstream cylinder respectively. During all this development of secondary shear layers, flow regime remains the same i.e. SS-I. Pictorial representation of secondary shear layers for all gap ratios is provided in Figure 3-16.

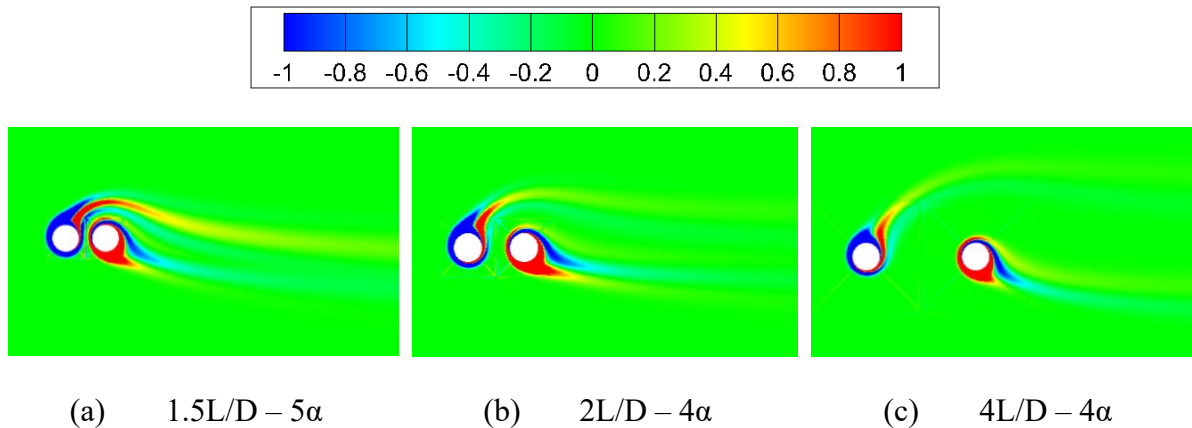


Figure 3-16 Vorticity contours representing secondary shear layers for different gap ratios

It is also observed that the length of shear layers in the wake of upstream cylinder is more at lower gap ratios in comparison to the high gap ratio values as with the increase in gap ratio the facilitation to the upstream cylinder shear layers because of downstream cylinder rotation reduces, thus reducing the overall length of the shear layers in the wake.

#### 3.2.4 Steady - wrapped combined flow (SS-I&II)

Comparing to the co-rotating cylinders study, an additional flow regime observed with counter rotating cylinders analyses at  $2L/D$  i.e. steady - wrapped flow where both the steady state – I and steady state II are observed simultaneously and thus referred as SS-I&II. In this flow regime the shear layers of upstream cylinder under the influence of the upcoming flow shed from the upper surface of the cylinder and traveling from above the downstream cylinder make the overall wake of the system. Meanwhile, the shear layers of downstream cylinder **which are not under active influence of the incoming flow**, start wrapping around the cylinder. Cylindrical rotation of the upstream cylinder also facilitates this wrapping of shear layers around the downstream cylinder. It is important to notice that unlike the conventional SS-I regime, in this case the positive shear layers from the upstream cylinder are at the top whereas the negative shear layer after wrapping around the upstream cylinder shed from underneath the positive shear layer. Pictorial representation for SS-I&II flow regime is done in Figure 3-17.

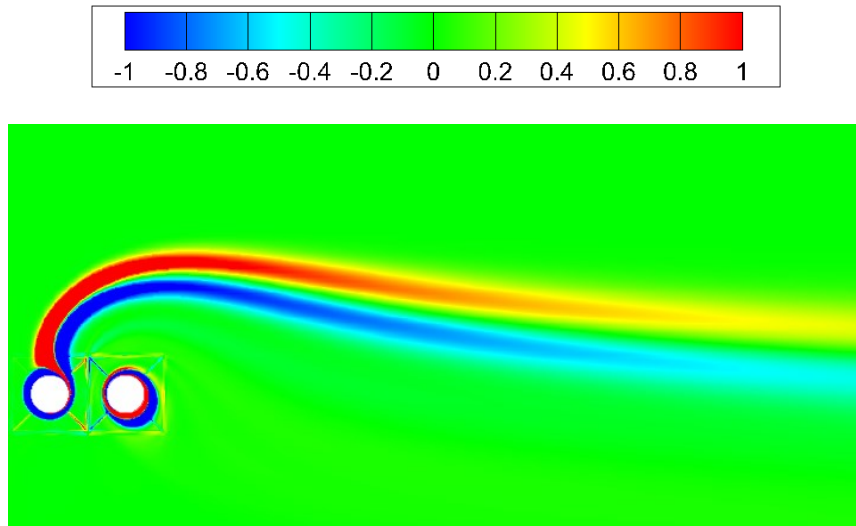


Figure 3-17 Vorticity contour for SS-I&II flow regime for 2L/D at  $9\alpha$

This flow regime is only observed in cases where there is an appropriate gap in between the cylinder, allowing the shear layers of the downstream cylinder to wrap around the cylinder and thus this flow regime is not observed in case of 1.5 L/D and 4 L/D. In case of 1.5 L/D the gap in between the cylinders is too less to allow the wrapping of shear layer around the downstream cylinder whereas in 4 L/D case the gap between the cylinders is large enough that upcoming flow impact on the downstream cylinder becomes significant and the flow directly shift from the steady to unstable flow state where both the cylinders start shedding secondary vortices at the same time. But for 2 L/D the fully developed secondary unstable flow does not occur as the flow shifts from the SS-I&II flow state to secondary unstable – wrapped flow with secondary vortical shedding only from the upstream cylinder as described in the next section.

### 3.2.5 Secondary Unstable flow

Secondary unstable single bluff body flow for the counter rotating cylinders is subdivided into 2 main categories. First when the secondary vortices only shed from the upstream cylinder and flow remain wrapped around the downstream cylinder referenced as secondary unstable – steady state II flow (SU-SS-II). Secondly when both the cylinders undergo unstable state simultaneously and shed secondary vortices separately. This flow state is termed as secondary unstable - inverted rotation flow (SU-IR).

#### 3.2.5.1 Secondary Unstable – Inverted Rotation flow (SU-IR)

For counter rotating cylinders, the SU-IR flow is observed only in case of 4L/D where the gap in-between both the cylinders is adequate to allow the formation and shedding of



secondary vortices from both the cylinders separately. This flow regime continues from  $5.25 - 5.5\alpha$  to  $6.125 - 6.15625\alpha$  during which there is shedding of secondary vortices from both the cylinders in opposite directions. The upstream cylinder sheds vortex above the system whereas the downstream cylinder sheds the vortex below the overall system. During this phase, it is also noticed that irrespective of changes in the  $\alpha$ , the separate vortices shedding from both the cylinders remain in-sync with each other. In previous literature this flow regimes is mostly referenced as Inverted Rotation (IR) flow [15].

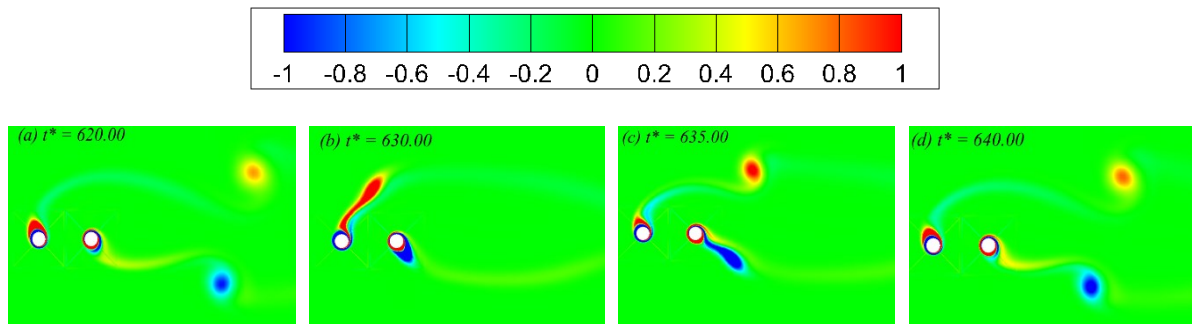


Figure 3-18 Vorticity contours showing SU-IR flow regimes for  $4L/D$  at  $5.5\alpha$

### 3.2.5.2 Secondary unstable - wrapped flow (SU-SS-II)

At the gap ratio of  $2 L/D$  increasing the  $\alpha$  value under SS-I&II flow regime, the upstream cylinder starts on shedding the secondary vortices but the downstream cylinder have shear layers wrapped around it. Hence this flow regime is referred as secondary unstable – wrapped flow state (SU-SS-II). Figure 3-19 shows the time streak for vortex shedding of SU-SS-II flow regime. Clear shedding of single strong vortex from upstream cylinder and wrapping of shear layers on the downstream cylinders can be seen in Figure 3-19. This flow regime is not observed in case of  $1.5 L/D$  and  $4 L/D$  where secondary vortices start shedding from both the upstream and downstream cylinder simultaneously. For  $2L/D$  this flow regime starts around  $11.25\alpha$  and terminates near  $14.875\alpha$ .

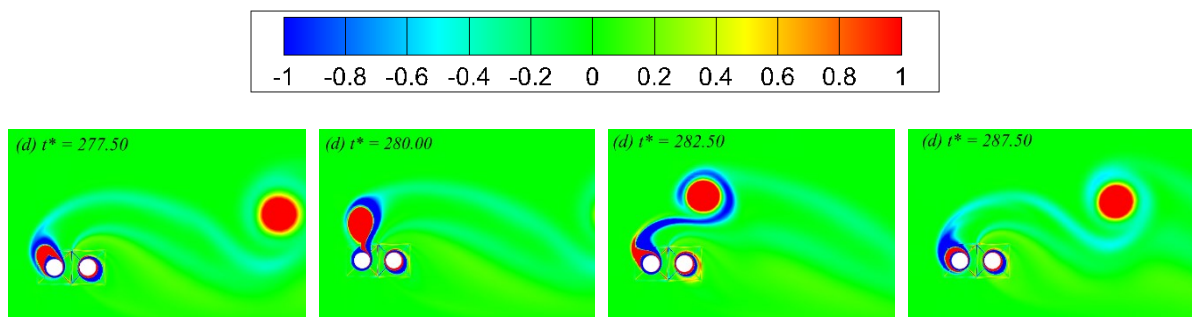


Figure 3-19 Vorticity contours demonstrating SU-SS-II flow state for  $2L/D$  at  $12\alpha$

### 3.2.6 Secondary stable flow (SS - II)

With further increase in angular rotation applied to both the cylinders, the shear layers start wrapping around both the cylinders independently. Like co-rotating cylinders analyses, this flow regime is termed as the secondary stable flow SS-II, further increment in the angular rotation to cylinders do not cause any significant change in flow state, only the shear layers becomes more strengthen and advance closer to the surface of the cylinder. For  $2L/D$  and  $4L/D$  this flow regime is observed above  $14.9375\alpha$  and  $6.15625\alpha$  respectively. Depending upon the rotation sense the recirculation zone of the extended shear layer is different for both the cylinders as evident from the Figure 3-20.

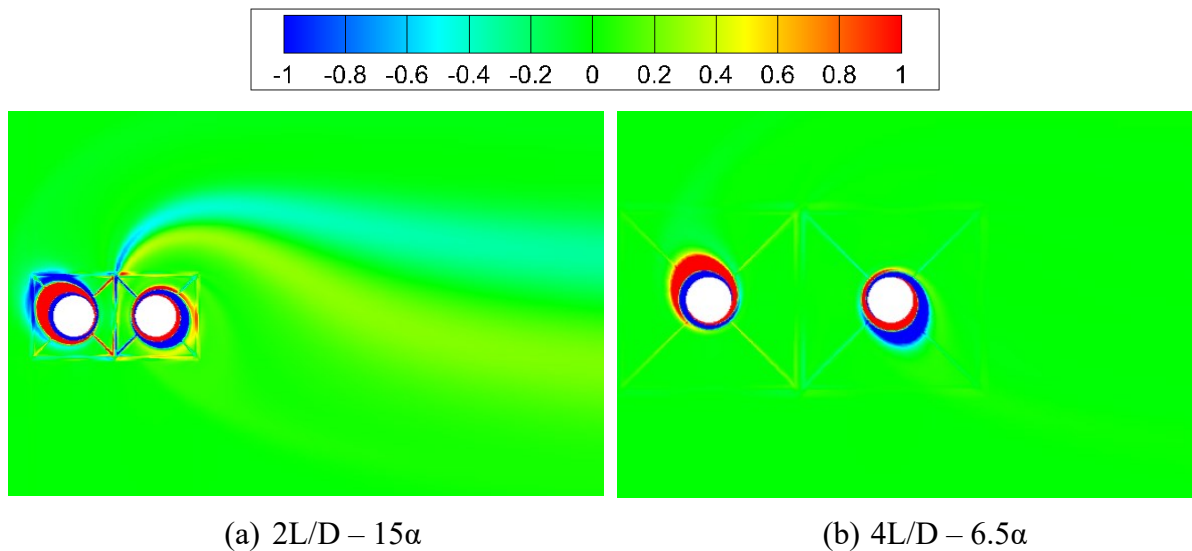


Figure 3-20 Vorticity contours for SS-II flow state at different gap ratios

## CHAPTER 4: STAGNATION POINTS

In the present study the stagnation points around the cylinder are traced using averaged velocity streamline about the cylinders, and the corresponding effect on lift and drag characteristics of whole system is related.

The generic trend observed in most of the cases with respect to stagnation points is that: stagnation points are closest to the cylinder surface in the steady flow without any angular rotations and as the angular rotation  $\alpha$  is applied to the cylinders, not only the stagnation points start to merge with each other and displace along the cylinder surface but also move away from the cylinder surface in radial manner and subsequently result in elevated magnitude of force coefficients.

### 4.1 Gap ratio 1.5 L/D

For 1.5 L/D, starting with the application of slight angular rotation  $\alpha$  i.e.  $0.5\alpha$  there are three stagnation points. One above the upstream and downstream cylinder each and one in between both the cylinders as shown in the pictorial representation Figure 4-1 (a), (b). With increase in  $\alpha$  the stagnation points in between both the cylinders remain there but the one above the upstream cylinder starts to progress towards the upper surface against the rotation direction. Which is in accordance with the literature and theoretical study as the movement of stagnation point is depicted by the elevation in pressure of the local region. And thus, the overall lift coefficient in downward direction increases in magnitude.

But as  $\alpha$  is increased further, in between  $3 - 4 \alpha$  the stagnation points of upstream cylinder and one in the gap **merge** with each other forming single stagnation point and the stagnation point of the downstream cylinder keeps on progressing outward from cylinder surface Figure 4-1 (c), (d). Further increase in  $\alpha$  only results in the movement of saddle point away from the cylinders along with adjusting itself in the middle of the system in horizontal manner Figure 4-1 (e), (f). Overall resulting in the increase in lift coefficient.

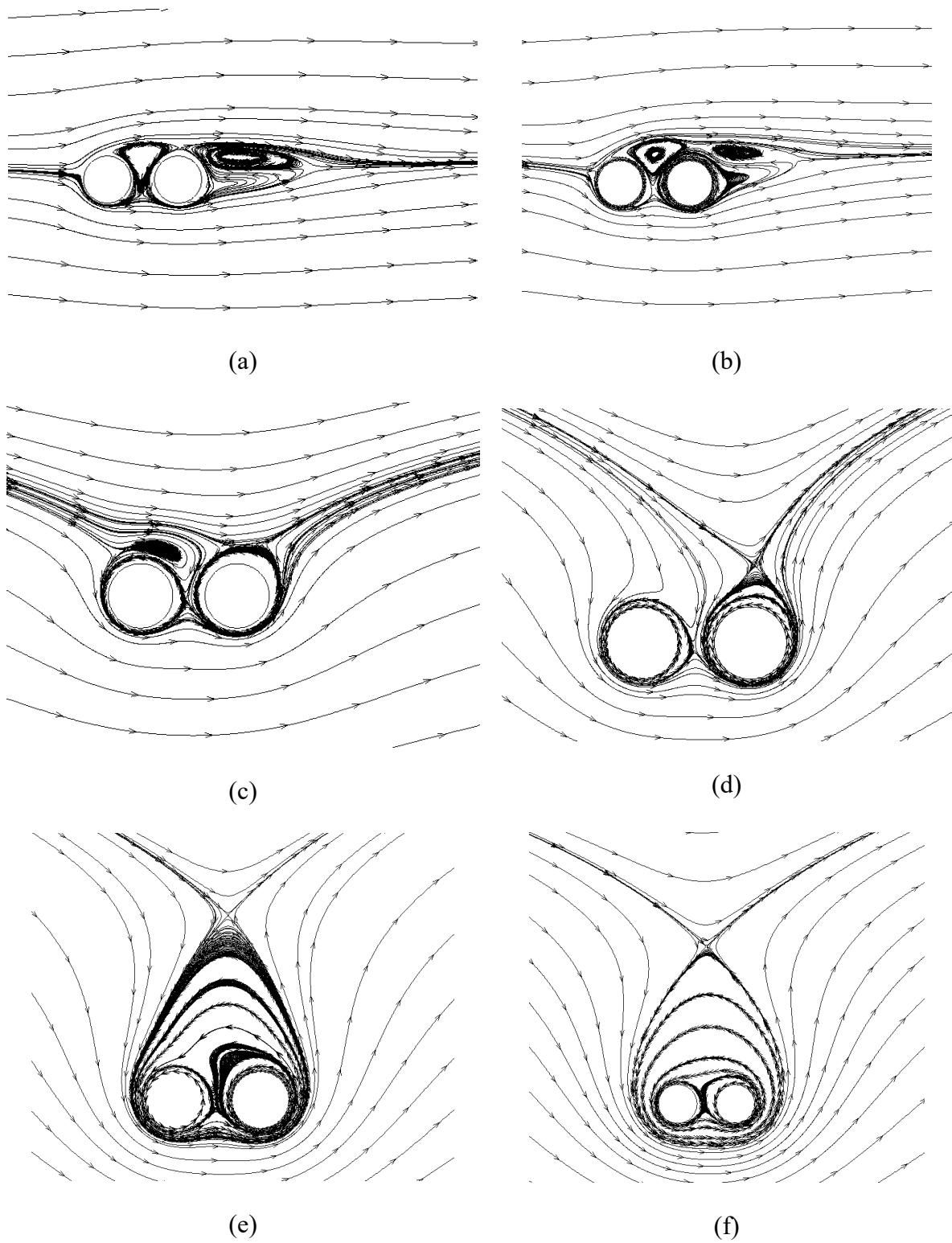
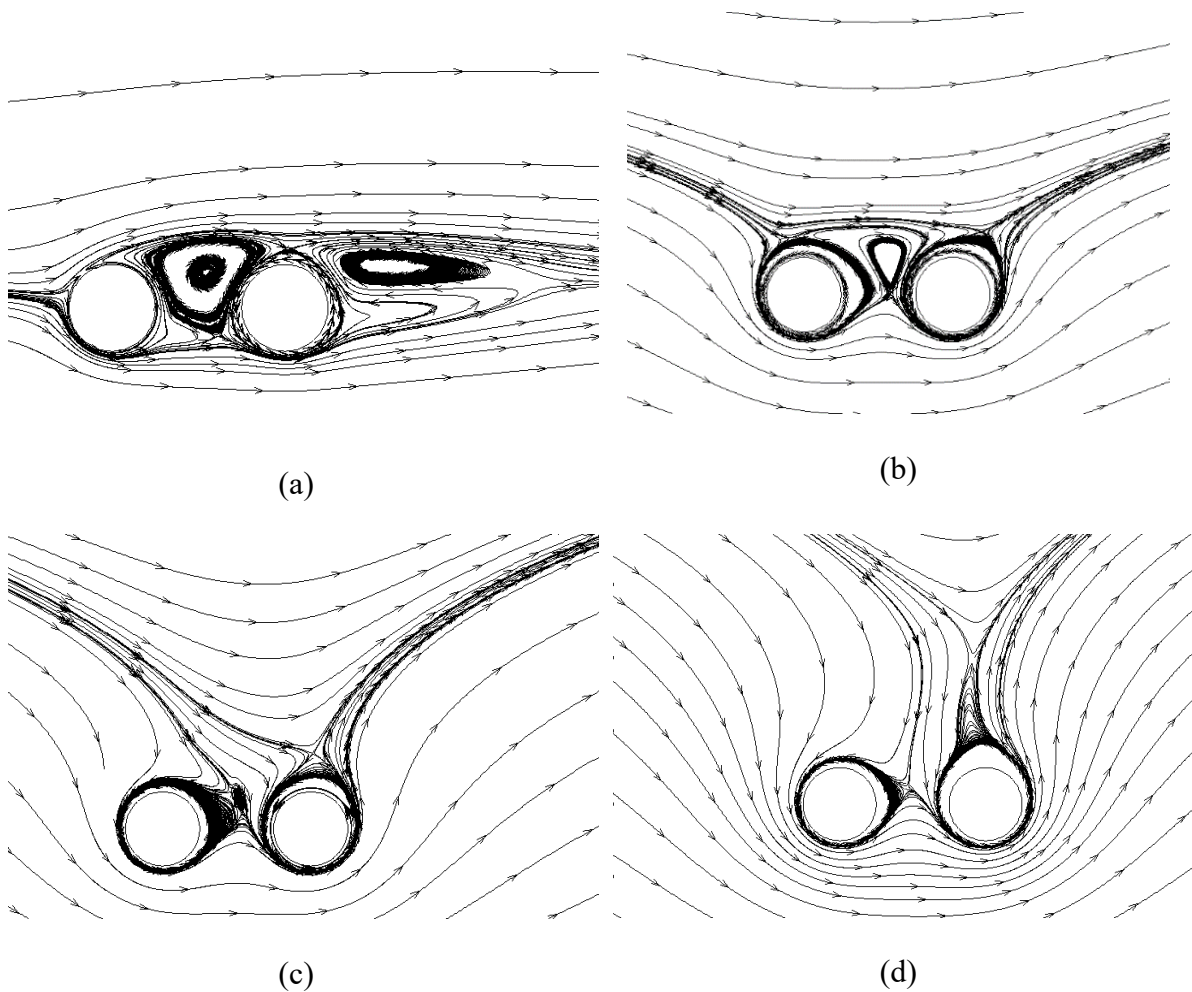


Figure 4-1 Tracing of stagnation points (a)  $0.5\alpha$  – total 03 stagnation points (b)  $1\alpha$  (c)  $3\alpha$  (d)  $4\alpha$  – merging of two stagnation points (e)  $5\alpha$  (f)  $6\alpha$  – relative movement of stagnation points away from the cylinders surfaces with increasing  $\alpha$ .

## 4.2 Gap ratio 2 L/D

Now for 2 L/D, we see a noticeable impact of gap ratio over the movement of stagnation points with the alteration of  $\alpha$ . With the application of slight  $\alpha$ , a total of 03 stagnations points show up with one in the gap between cylinders and one above each cylinder. Increase in  $\alpha$  cause the stagnation point over the upstream cylinder to move along the cylinder surface opposite to the angular rotation as anticipated and the stagnation point over the downstream cylinder moves along the cylinder surface in the direction of rotation thus compensating the overall pressure variation in flow field, thus both coming closer to each other. But stagnation point of upstream cylinder shows more sensitivity towards rotation and around  $4\alpha$  it comes quite close to the stagnation point in between the two cylinders. And finally merge with it at around  $4.5\alpha$ . now with further increase in the  $\alpha$ , the stagnation point in the middle remains at the same place but that of downstream cylinder moves away from the cylinder surface as shown in the pictorial representation Figure 4-1.



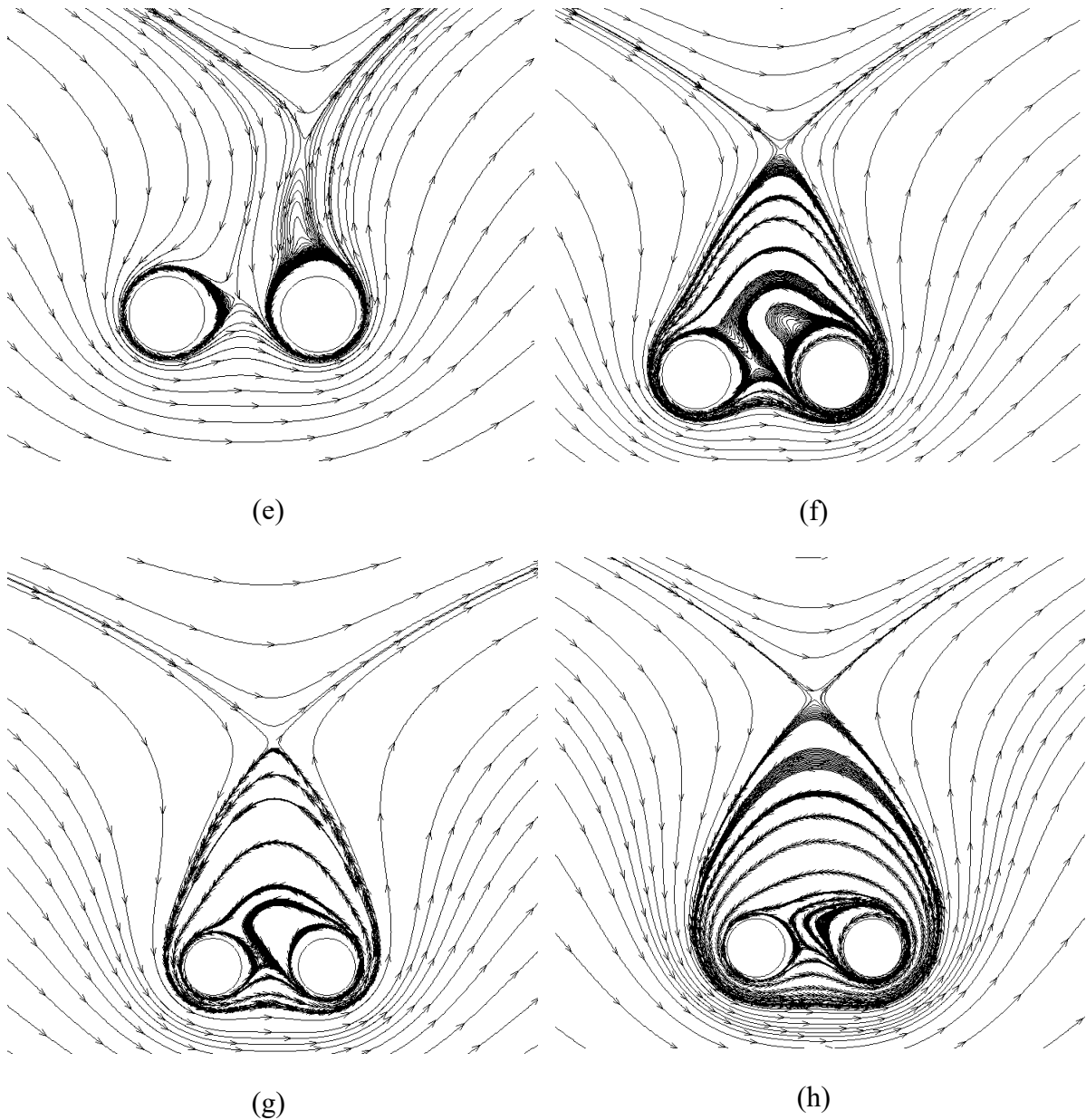


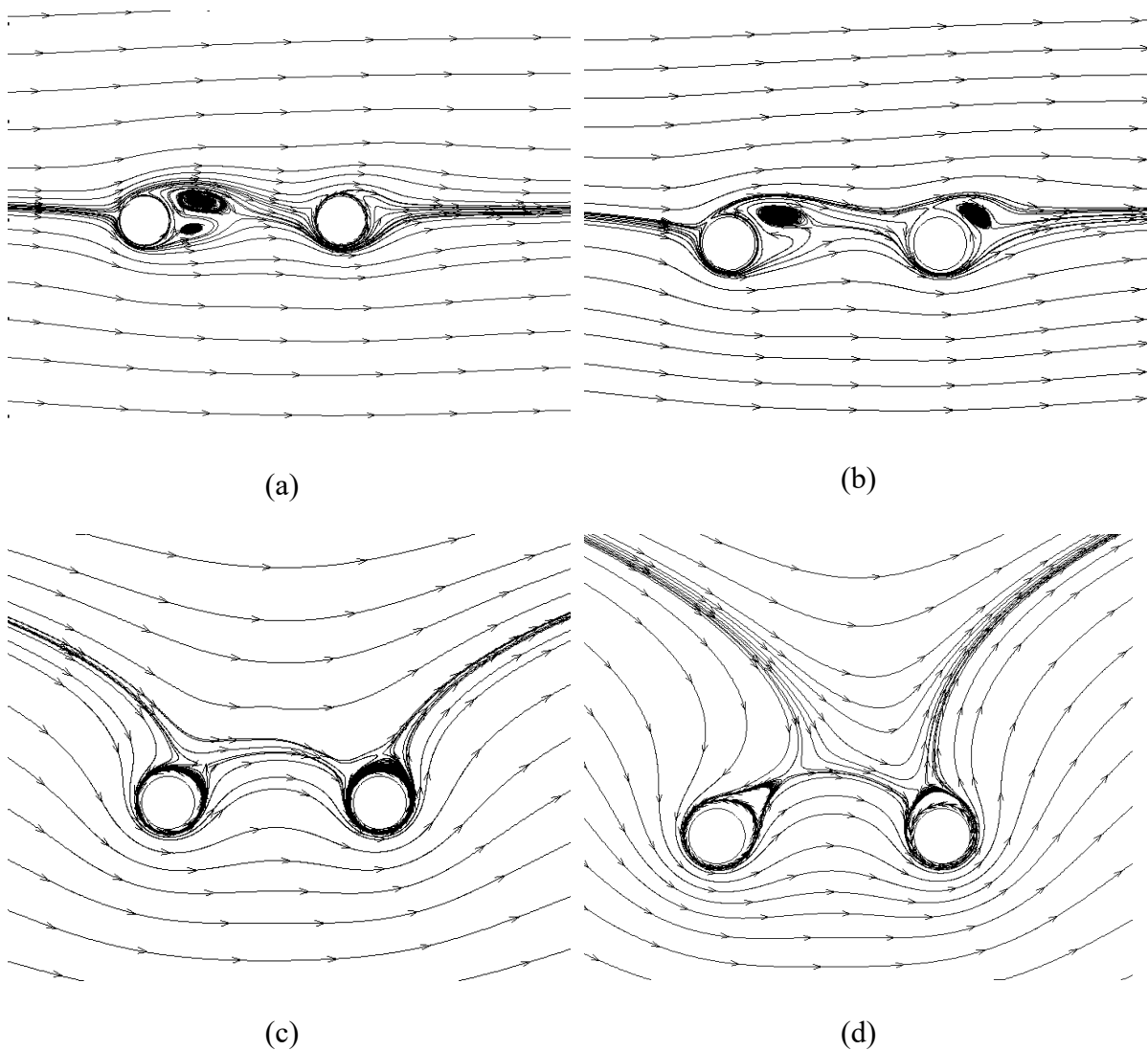
Figure 4-2 Stagnation point tracing 100 Reynold number 2 L/D (a)  $0.5\alpha$  - 03 stagnation points (b)  $3\alpha$  - stagnation points moving closer to each other (c)  $4\alpha$  - two stagnation points about to merge (d)  $4.625\alpha$  - overall two stagnation points (e)  $4.71875\alpha$  - downstream stagnation point moving away from cylinder surface (f)  $5\alpha$  saddle point moving away (g)  $5.46875\alpha$  (h)  $6\alpha$

### 4.3 Gap ratio 4 L/D

For 4L/D flow around the cylinder shows much similarity to single cylinder flow. The vortices from both the upstream and downstream cylinder shed separately. Therefore, at lower rotation rates, there are several stagnation points rather than only two to three as in the case of lower gap ratio. The prominent stagnation points are traced in the study.

Starting from slight  $\alpha$  of 0.5, there is one main stagnation point above each cylinder, and other saddle points are along the vortices shedding from both the upstream and downstream cylinders. Increasing the  $\alpha$  causes the asymmetry in the shedding vortices developing over both the cylinders. Also, the stagnation point of upstream cylinder moves along the surface counter to the rotation direction to balance the pressure differential, whereas the stagnation point of downstream cylinder moves forward in the direction of rotation as it is effected more by the  $\alpha$  because it is not under much influence of upstream flow. With further augmentation in  $\alpha$ , stagnation points of both cylinders move away from the cylinder surfaces and ultimately merge with each other making wrapping flow in which one stagnation point is in the wrapped shear layers and the other one is above the overall envelope of shear layers.

Respective movements and merging of stagnation points for 100 Reynold number and 4 L/D are pictorially represented in Figure 4-3.



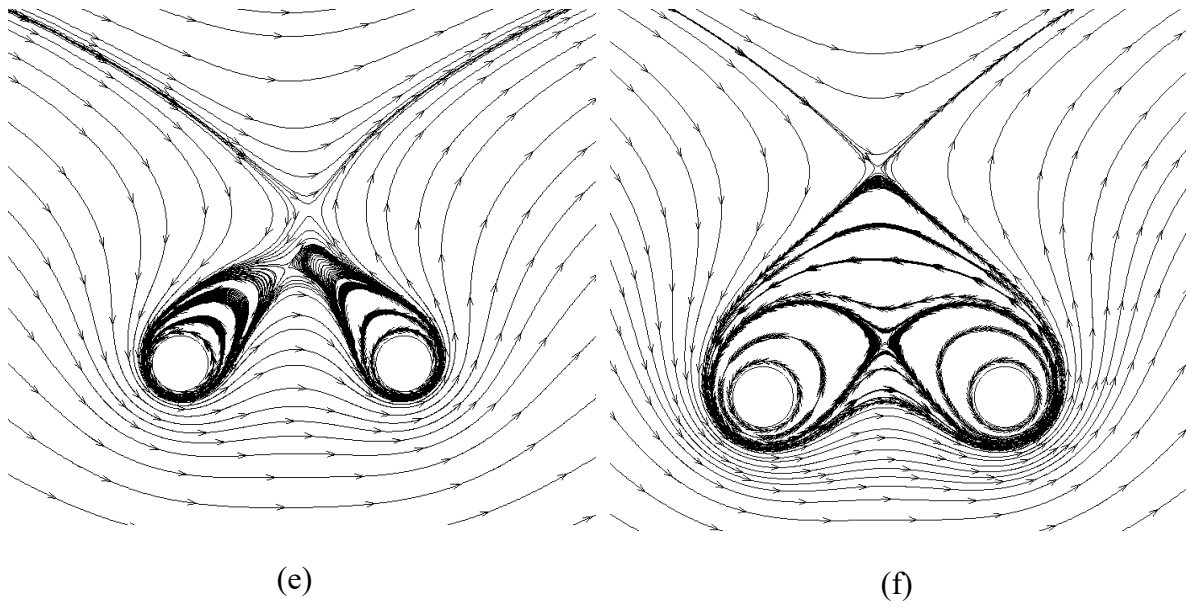


Figure 4-3 Movement of stagnation points 100 Reynold number -  $4L/D$  (a)  $0.5\alpha$  (b)  $1\alpha$  (c)  $4\alpha$  (d)  $5\alpha$   
 (e)  $5.25\alpha$  (f)  $6\alpha$



## CHAPTER 5: LIFT AND DRAG COEFFICIENTS VARIATION AT 100

### REYNOLDS NUMBER FOR VARYING ALPHA AND L/D

Tandem arrangement of two rotating cylinders offers diverse flow regimes for variation of both the  $\alpha$  and L/D as mentioned in the preceding sections. This section deals with the variation of force coefficients in these flow regimes while altering the control parameters i.e.,  $\alpha$  and L/D. Section is subdivided in an orderly manner. As the nature of fluid flow varies depending upon the rotation orientation, hence explanation is done for co-rotation and counter rotation of cylinders separately.  $\alpha$

#### 5.1 Force coefficients for co-rotation

Both the cylinders are made to rotate in the counterclockwise direction, along with alteration in gap ratios and  $\alpha$ . Based on the  $C_D$  results, under same rotation direction, both the cylinders tend to push each other apart.

##### 5.1.1 Gap ratio 1.5 L/D

For a constant gap ratio of 1.5 L/D with the increase in  $\alpha$ , it is observed that magnitude of  $C_L$  for the upstream cylinder increases as shown in Figure 5-1. During this shift the primary and secondary vortical structures shed from the system but the overall rate of increase of  $C_L$  does not alter. Similar trend is shown by the  $C_L$  of the downstream cylinder. Considering  $C_D$ , with increase in the rotation rate the  $C_D$  of the upstream cylinder decrease in a delayed quadratic manner, starting from a very small positive value of 1.17,  $C_D$  then first gets zero at around  $\alpha = 2$  and then decrease to negative value of -29.1797 for 6  $\alpha$  (non-dimensional rotation rate). ***Reason for the negative drag can be associated with the increased pressure region in between the two cylinders indicating the presence of stagnation point because of opposite flow direction under the influence of counter rotating cylinders, eventually pushing the upstream and downstream cylinders in the forward and backward directions respectively. And thus, both the cylinders show repulsive characteristics, pushing each other in opposite directions as shown in*** Figure 5-2. Magnitude of drag for both the cylinders show an increasing trend with increase of  $\alpha$ , starting from almost 0 to a drag coefficient of approximately 30 for nondimensional  $\alpha = 6$ . Considering overall flow parameters, the combination of cylinders behaves more like a single bluff body as both the cylinders are placed quite close to each other.

Figure 5-1 also shows the transitions of flow regimes with gradual change of  $\alpha$ . For 1.5 L/D the secondary unstable stage of single bluff body vortical shedding is over very less  $\alpha$  range depicting the overall stable nature of the system.

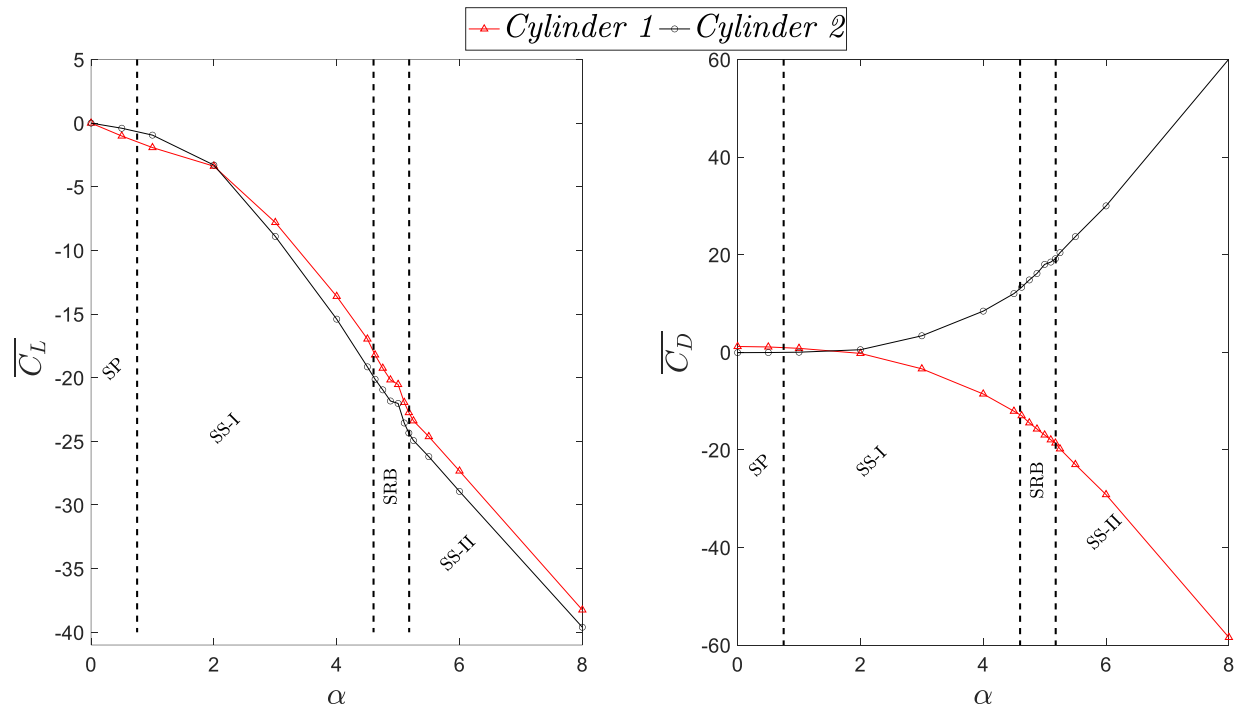


Figure 5-1 Mean lift and drag coefficients for upstream (Cylinder-1) and downstream (Cylinder-2) at 1.5L/D

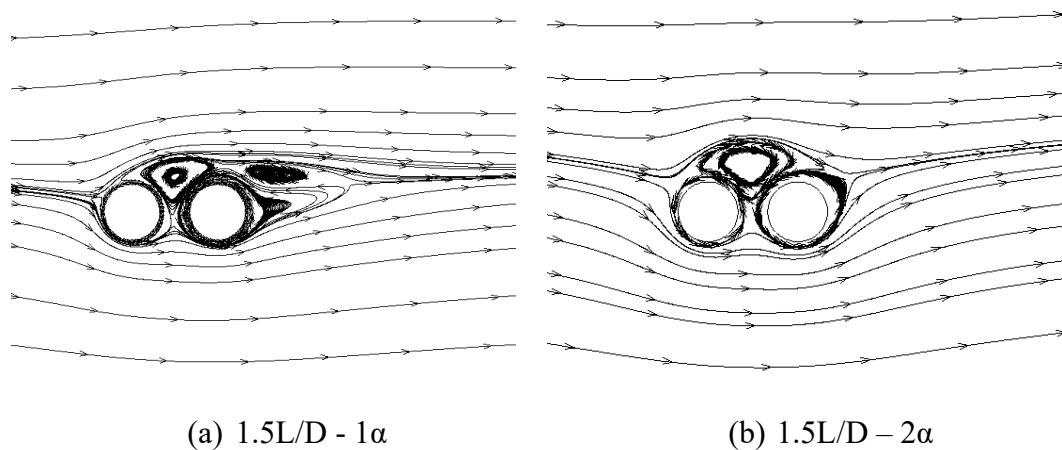


Figure 5-2 Time averaged flow field 2-D streamlines indicating stagnation point for co-rotating cylinders

The onset of secondary vortices is traced via  $\sigma$  graphs of  $C_L$  and  $C_D$  data from the corresponding mean values. The secondary vortices for 1.5 L/D center to center case start around  $4.5 - 4.625\alpha$  and ends in between  $5.175-5.2125 \alpha$ , as shown in the  $\sigma$  graph in Figure

5-3. Relative difference of magnitude between the primary unstable state of SP flow regime and secondary unstable state of SRB flow can be seen from  $\sigma$  graph. A peculiar notch is observed in SU-SRB flow regime for upstream cylinder, which depict the unstable and transitional flow nature in this regime. For both the  $C_L$  and  $C_D$   $\sigma$  graphs of upstream and downstream cylinders, deviation of upstream cylinder is observed to be approximately half compared to the downstream cylinder. With the development of the shedding vortex, it is observed that the positive shear layer expanding over both the cylinders first accumulates over the downstream cylinder under the influence of the upstream flow. The vortex shedding then takes place from the region above the downstream cylinder. Hence amplifying the impact of force coefficients over downstream cylinder relative to the upstream cylinder. Hence in the  $\sigma$  graphs, cylinder 2 deviation from the means values is noticed to be more in comparison to cylinder 1.

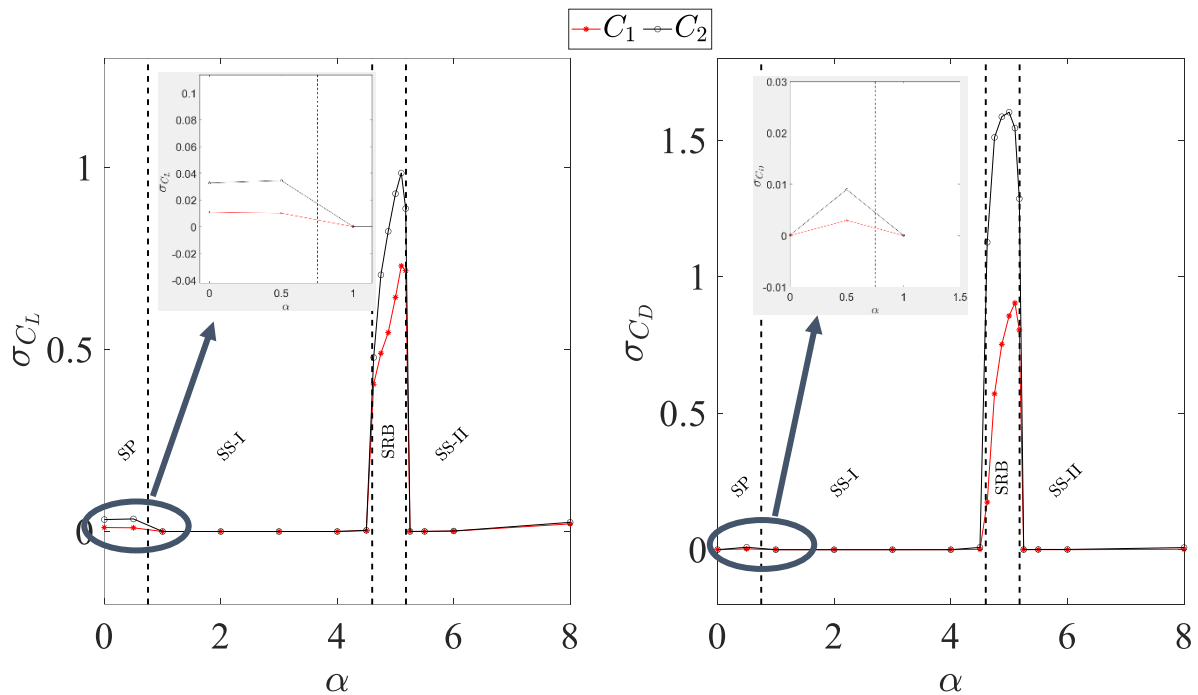


Figure 5-3  $C_L$  and  $C_D$   $\sigma$  vs  $\alpha$  range plot for 1.5 L/D – Upstream cylinder 1, downstream cylinder 2

### 5.1.2 Gap ratio 2 L/D

At 2 L/D for same orientation of rotation, as the  $\alpha$  is increased the variation in the  $C_L$  and  $C_D$  shows the same quadratic trend as that for 1.5 L/D.  $C_L$  for the upstream cylinder starts from 0 and ends at approx. 28.77 for  $\alpha = 6$ . Similarly, the  $C_L$  for downstream cylinder starts from 0 and gives 30.81 for  $\alpha = 6$ . It is noticed that following the similar trend as for 1.5L/D

gap ratio, the  $C_L$  is higher for upstream cylinder for the  $\alpha$  range of 0 to 3, but with further increase in  $\alpha$  downstream cylinder shows higher  $C_L$  values.

$C_D$  in case of 2 L/D shows quite smooth variation curves, for upstream cylinder it starts from 1.14 at 0  $\alpha$  and ends at -27.70 for 6 $\alpha$ . Negative sign with the  $C_D$  of upstream cylinder shows that the cylinder faces upstream directed force owing to the pressure increase between the cylinders due to opposite flow direction in between both the cylinders like 1.5L/D cases. Transition of  $C_D$  for upstream cylinder from positive to negative value occurs in between 1-2 $\alpha$  range when the impact of downstream cylinder rotation become significant in the region between both the cylinders. Corresponding mean  $C_L$  and  $C_D$  plots are shown in Figure 5-4.

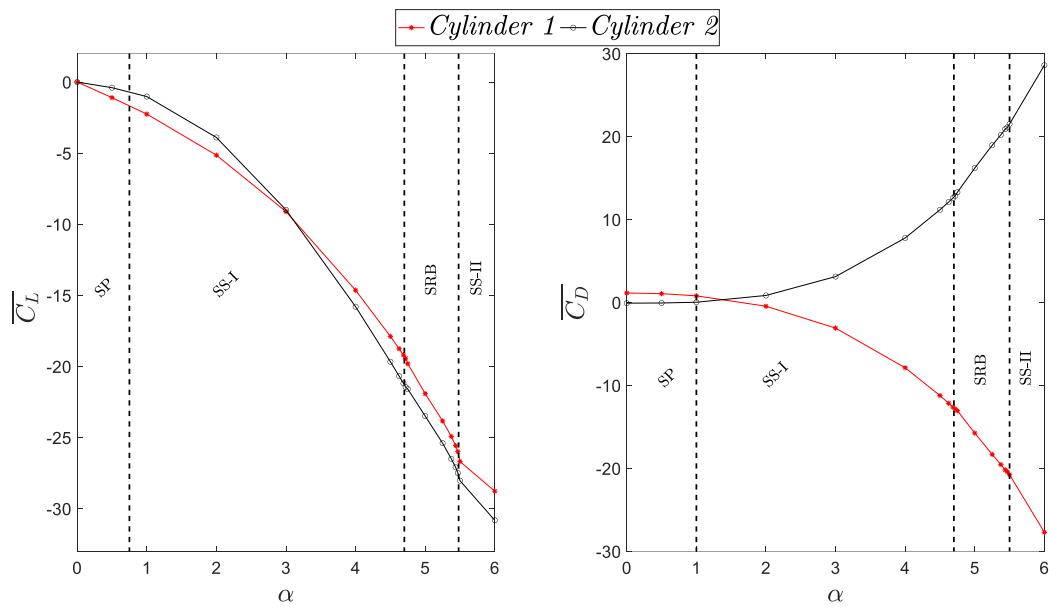


Figure 5-4 Mean lift and drag coefficients for upstream (Cylinder-1) and downstream (Cylinder-2) at 2L/D

$\sigma$  plots for 2 L/D are provided in Figure 5-5. Secondary vortices start in between 4.6875/4.71875 and end in between 5.46875/5.5. In comparison to the 1.5 L/D case the secondary vortices regime is shifted at a higher  $\alpha$  i.e., secondary vortices are starting and ending at higher  $\alpha$  values. It is important to mention that the magnitude of standard deviation of  $C_L$  is same for both the upstream and downstream cylinder but for  $C_D$  upstream cylinder  $\sigma$  value is 1.05 and downstream cylinder  $\sigma$  value is 1.78, approximately 80% more than that of the upstream cylinder. Reason: as the downstream cylinder is not under the direct influence of upstream flow hence the overall drag on downstream cylinder owing to the SRB regime vortex shedding is more pronounced relative to the upstream cylinder.

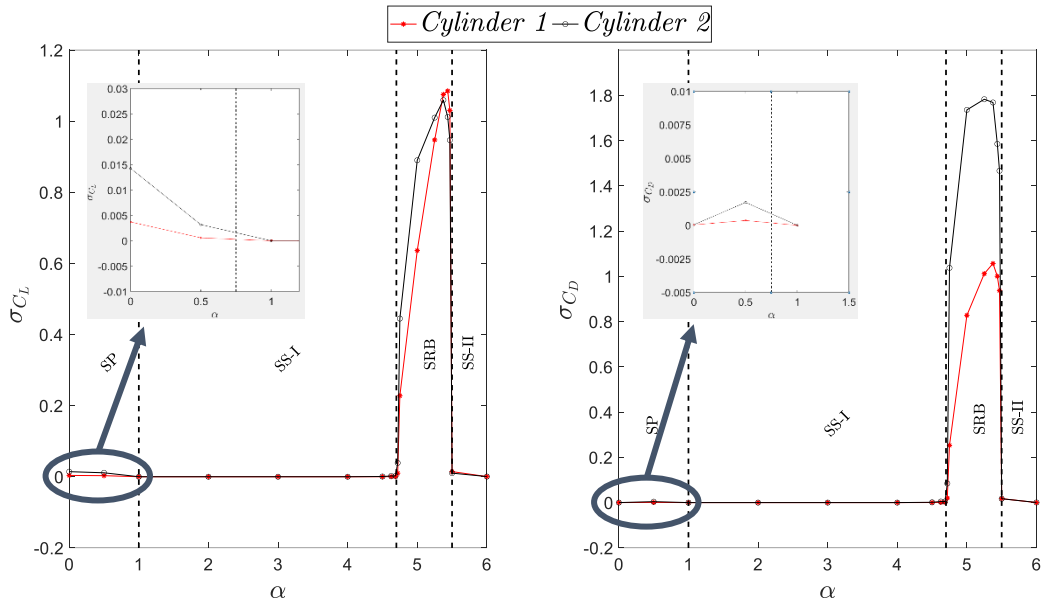


Figure 5-5  $C_L$  and  $C_D$  standard deviation vs  $\alpha$  range plot for 2 L/D – Upstream cylinder 1, downstream cylinder 2

### 5.1.3 Gap ratio 4 L/D

Mean force coefficient plots are provided in Figure 5-6. The magnitude of  $C_L$  and  $C_D$  for the upstream and downstream cylinders are comparable to each other.  $C_L$  of upstream and downstream cylinders starts from approx. 0, varies all the way up to 32.51 and 32.35 for  $6\alpha$  respectively.  $C_D$  for the upstream cylinder starts from 1.25 and ends at -19.53. For the downstream cylinder  $C_D$  starts from 0.68 and ends at 20.51 as depicted in the Table 5-1. Like the 1.5L/D and 2L/D, negative drag is also noticed for the upstream cylinder.

Unstable vortex shedding flow states are traced using  $\sigma$  plots for force coefficients. An important consideration is the increased oscillation magnitude for primary unstable state i.e. AC flow regime where primary vortices continue to shed for approx.  $\alpha = 2.5/3$  (nondimensional). AC flow regime observed here for 4L/D, is not noticed for 1.5 and 2 L/D gap ratios. Compared to the SP flow states observed at lower gap ratios the AC flow regime

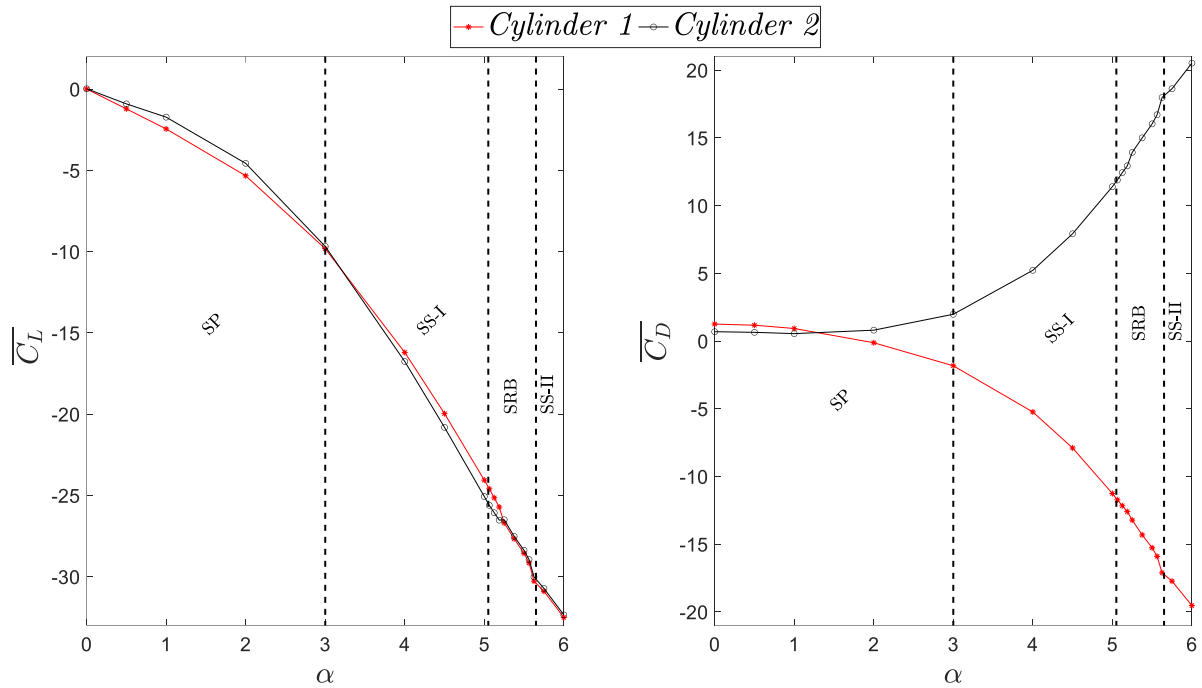


Figure 5-6 Mean lift and drag coefficients for upstream (Cylinder-1) and downstream (Cylinder-2) at 4L/D

demonstrates significantly higher  $\sigma$  from means force coefficients values. During the first unstable vortex shedding phase, extent of deviation of both  $C_L$  and  $C_D$  force coefficients for downstream cylinder is more compared to the upstream cylinder, because IAC flow here causes vortices to first shed from the upstream cylinder, falling on the downstream cylinder, resulting in more pronounced force coefficients.

Secondary vortices start from 5-5.125  $\alpha$  and end at 5.5625/5.625 $\alpha$ . Comparing from the 1.5 and 2 L/D simulation cases, the secondary vortices are further delayed, and the region of shedding is also narrowed. Whereas the downstream cylinder shows typical behavior of more  $\sigma$  of coefficients magnitude in comparison to the upstream cylinder, primarily because it's not under the direct influence of upstream flow.

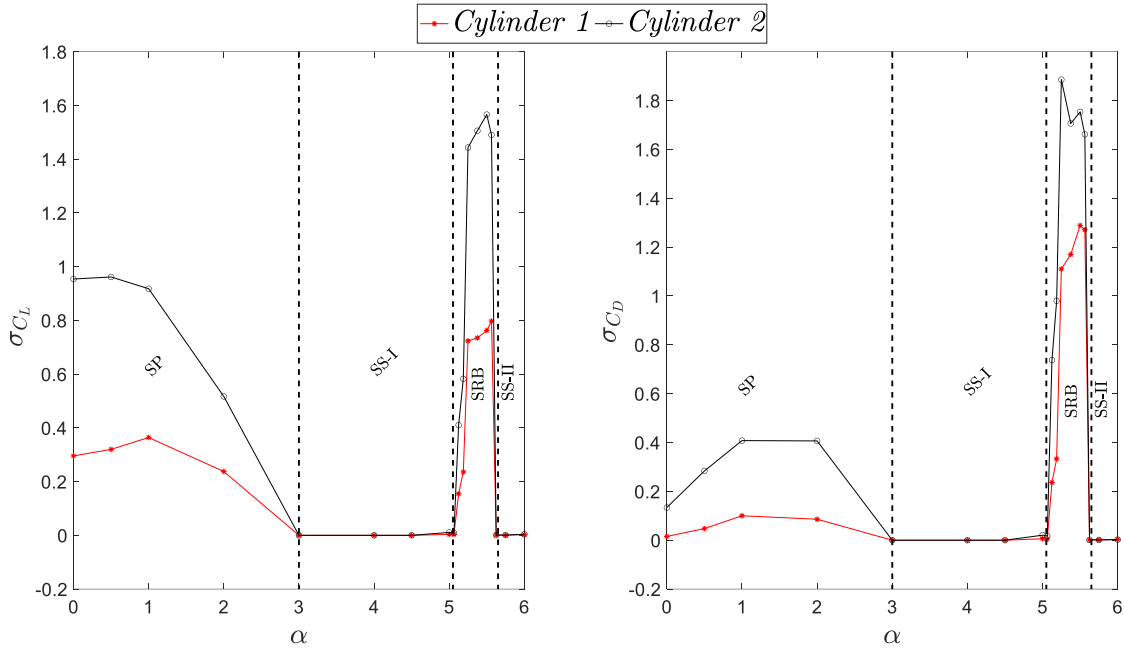


Figure 5-7  $C_L$  and  $C_D$  standard deviation vs  $\alpha$  range plot for 4 L/D – Upstream cylinder 1, downstream cylinder 2

Noticing the trend of force coefficients magnitude on increasing the L/D gradually from 1.5, 2 and 4, for both the upstream and downstream cylinders increase in  $C_L$  and decrease in  $C_D$  is observed. For a constant  $\alpha$  of 6, the variation of magnitude of lift and drag coefficient for different L/D values is shown in Table 5-1. Negative drag for the upstream cylinder decreases with the increase in the  $\alpha$  value. It shows that with increase in the gap ratio the high-pressure region in between cylinders is weakening continuously and diminishing the negative drag on the upstream cylinder.

Table 5-1 Force coefficients variation with different L/D at  $6\alpha$

L/D	Upstream cylinder		Downstream cylinder	
	$C_L$	$C_D$	$C_L$	$C_D$
1.5	27.3298	29.1787	28.9335	29.9866
2	28.7708	27.7052	30.8164	28.5968
4	32.5105	19.5311	32.3519	20.5197

An important point to consider here is that with the increased gap ratio both the cylinders behave more like independent single cylinders and the system trend to shift away from that of SRB flow state.

## 5.2 Force coefficients for counter rotation

For setup of counter rotating cylinders, upstream cylinder is made to rotate in counterclockwise sense and downstream cylinder is rotated in clockwise direction.  $C_D$  data shows that unlike the co-rotating case, when cylinders are made to rotate in opposite directions, they tend to pull each other.

### 5.2.1 Gap ratio 1.5 L/D

Force coefficients for the counter rotating cylinder at 1.5L/D are shown in Figure 5-8. Simulations are performed covering  $8\alpha$  range. It is noticed that unlikely the result of co-rotating cylinders the  $C_L$  values for both the upstream and downstream cylinder are different. Upstream cylinder shows lower magnitude of  $C_L$  in comparison to the downstream cylinder. With gradual increment of  $\alpha$ , first the  $C_L$  for upstream cylinder increases till  $7\alpha$  quantitatively giving 9.6703 value, then decreases providing 8.0854 value for  $C_L$  at  $8\alpha$ . Whereas the downstream cylinder shows quadratic increase in the  $C_L$ , reaching 33.8955 at  $8\alpha$ . Reason for the unequal  $C_L$  coefficients for upstream and downstream cylinders is related to the presence and alteration of the location of stagnation points upon change in  $\alpha$  values. For co-rotating cylinders the stagnation point is observed in the region between both the cylinders but for the counter-rotating cylinders, stagnation points for upstream and downstream cylinder approximately moves above and below the cylinder respectively, causing increase in the magnitude of  $C_L$  for downstream cylinder, at the same time pushing upstream cylinder in the downward direction. Corresponding visual representation is done using 2-D streamlines of time averaged flow field in Figure 5-9.

Respectively some authors have given corresponding explanation using shear layers concept, as the lower  $C_L$  magnitude for the upstream cylinder is because of the development of strong secondary negative shear layer which starts from the above the upstream cylinder, wraps around passing in between both the cylinders, shed in the overall system wake from above the downstream cylinder as demonstrated in Figure 3-16(a). The positive shear layer primarily gets restrained to only small portion on cylinder circumference. Hence profound presence of negative shear layer on both above and below the upstream cylinder, impact the pressure distribution around it, resulting in decrease of  $C_L$  coefficient. But simulations performed at higher  $\alpha$  values shows that the  $C_L$  value after  $8\alpha$  again start mounting up in magnitude.



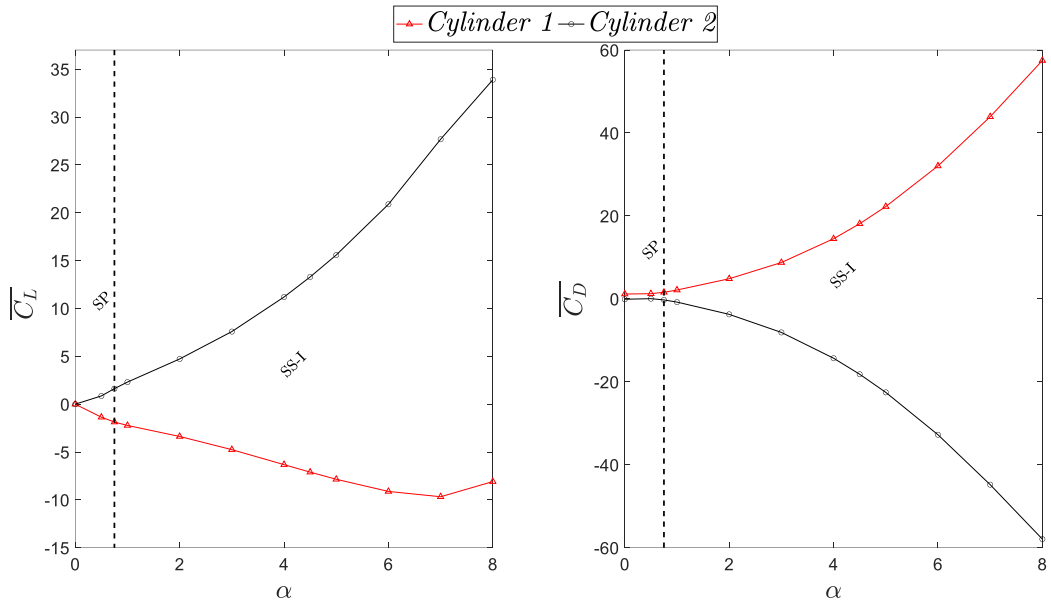


Figure 5-8 Force coefficients plot for 1.5L/D at different  $\alpha$

$C_D$  shows relatively plain coefficients plot where both the upstream and downstream cylinders show approximately similar force coefficients magnitudes at constant  $\alpha$  values except for direction of drag forces.

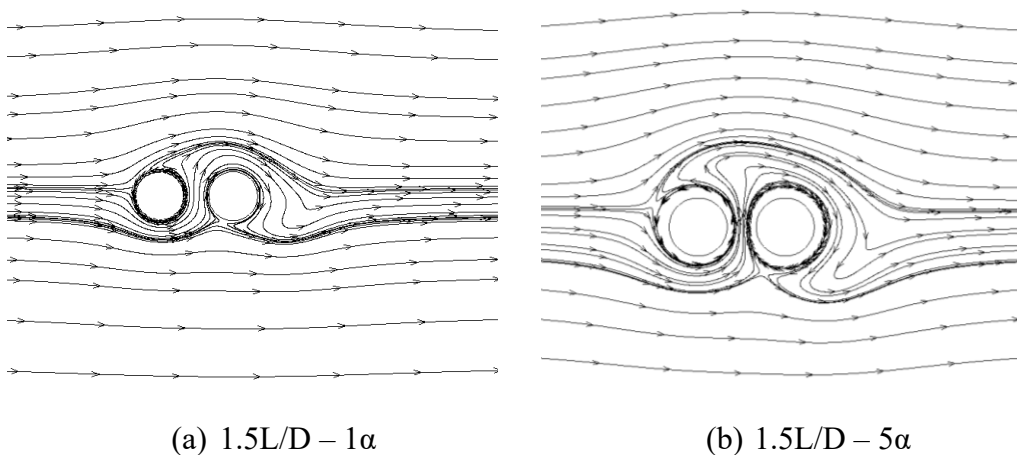


Figure 5-9 Counter-rotating cylinders flow field visualization via 2-D streamline

The reason for the attractive nature of both the cylinders in case of counter rotation application is the same as the repulsive nature for the co-rotating system. When cylinders are made to rotate in same orientation, the flow direction in between both the cylinder because of rotation is opposite to each other and stagnation point is observed in between them as shown in Figure 5-2. Whereas for the counter rotating cylinders the region in between both the cylinders experience increased flow velocity in upwards direction causing drop in pressure as

shown in Figure 5-9 with the help of 2-D streamlines. Thus, the drag on the upstream cylinder is positive and downstream cylinder is negative, causing both the cylinders to attract each other.

The unstable flow range for 1.5L/D counter rotating system of cylinders is traced using  $\sigma$  plots as shown in Figure 5-10. It is important to notice that for counter-rotating system of two cylinders at 1.5L/D, only SP and SS-I flow regimes are observed. There is no development of secondary vortices and thus secondary unstable state. Also, the  $\sigma$  magnitude of lift and drag coefficients is also very trivial in comparison to the  $\sigma$  values at co-rotating cylinder systems. With further increase in  $\alpha$ , only steady flow is noticed with proportionally increasing magnitude of force coefficients.

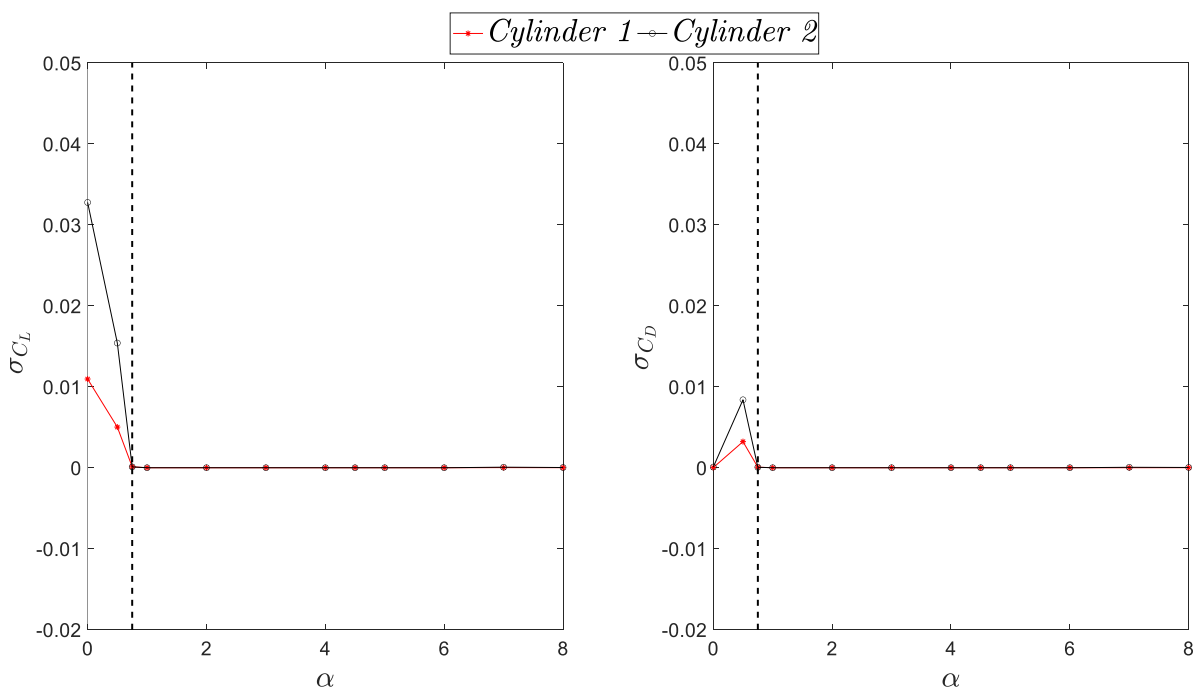


Figure 5-10 Counter rotating cylinders  $\sigma$  plots of force coefficients from mean position for 1.5L/D

### 5.2.2 Gap ratio 2 L/D

Multiple flow regimes are noticed when the tandem arrangement of two cylinders is made to rotate in opposite directions. Corresponding lift and drag coefficients along with flow regimes subdivision on the coefficient plots are provided in Figure 5-11. In comparison to all the rotating cylinder combinations in the current study this flow regimes extends to maximum  $\alpha$  along with two new flow regimes termed as SS-I &II and SU-SS-II flow. Corresponding explanation regarding flow regimes is done in FLOW REGIMES CLASSIFICATION.

Directions of force coefficients are identical to 1.5L/D analyses with both cylinders pulling each other.

In case of 2L/D at higher  $\alpha$  values while transitioning from stable to unstable flow regime only the upstream cylinder starts shedding vortices whereas the flow remains wrapped around the downstream cylinder for SU-SS-II regime. During this transition slight notch can be observed in the  $C_L$  and  $C_D$  graphs.  $\sigma$  graphs for 2L/D maps the secondary unstable range provided in Figure 5-12. Considering the magnitude of deviation from means position in comparison to 1.5 and 4L/D, 2L/D case shows exceptionally higher values.

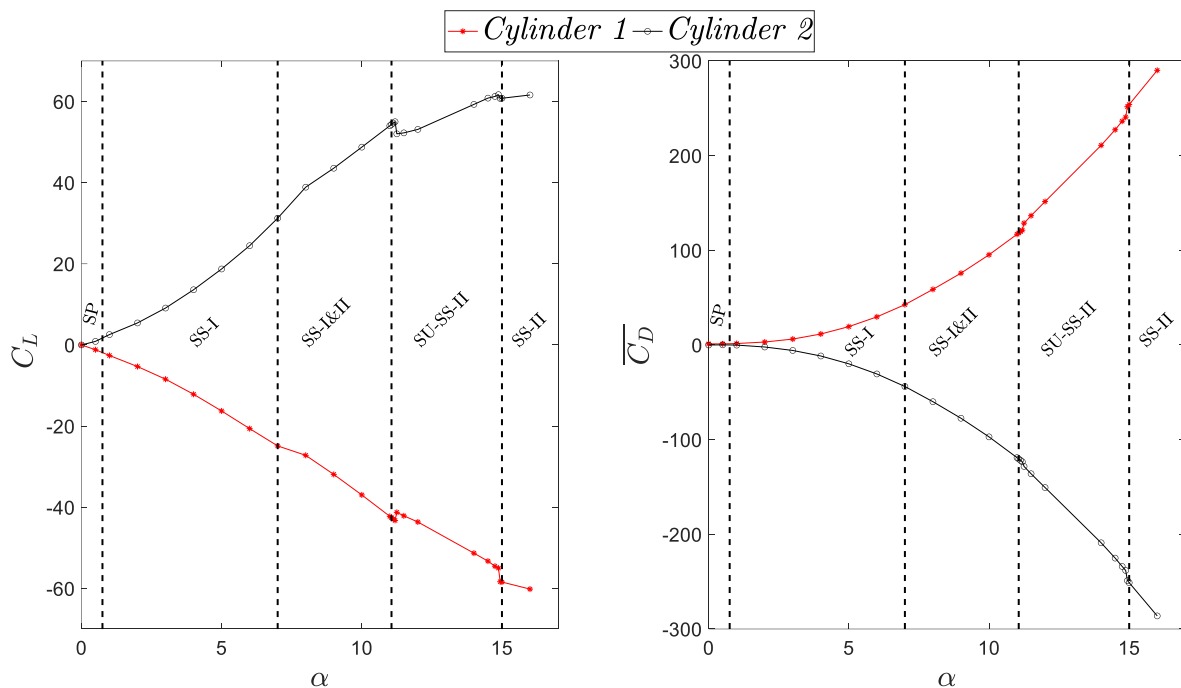


Figure 5-11 Mean force coefficient for counter rotating cylinders at 2L/D

For the secondary unstable state, the vortex shedding is taking place from the upstream cylinder thus the impact of secondary vortex shedding on the upstream cylinder is observed to be more pronounced in comparison to the downstream cylinder. Moreover, the comparison of magnitude of  $\sigma$  values for primary instable state i.e. PS flow regime and the secondary instable state i.e. SU-SS-II state is also demonstrated in the Figure 5-12.

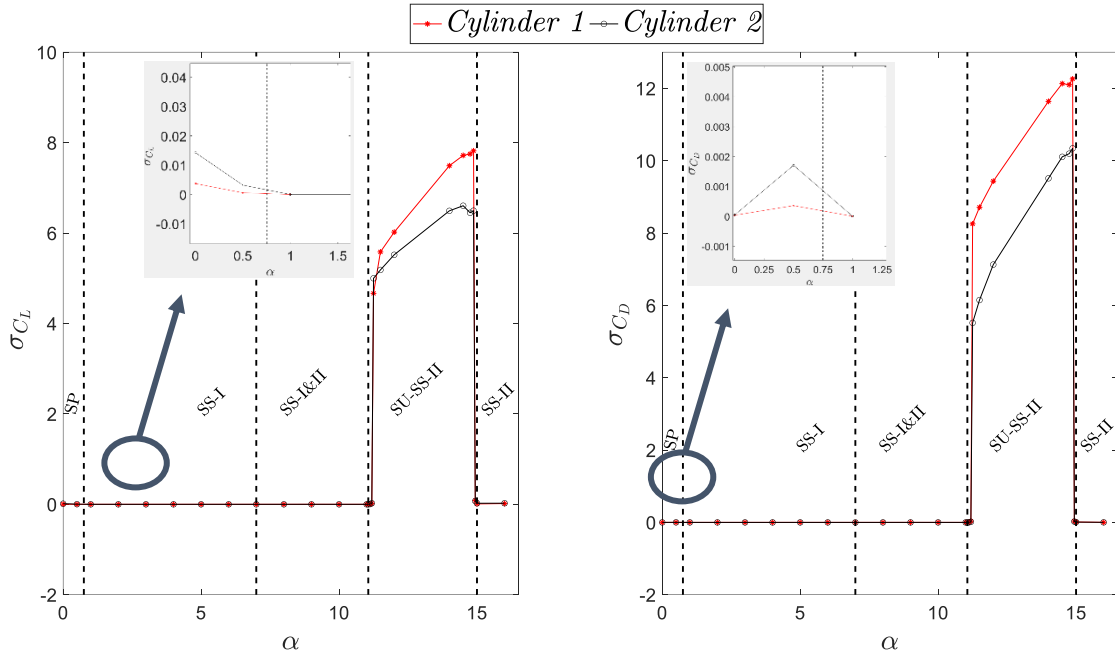


Figure 5-12  $\sigma$  plots for counter rotating cylinders at  $2L/D$

### 5.2.3 Gap ratio $4L/D$

Direction for lift and drag forces for the upstream and downstream cylinders remain same as for  $1.5L/D$  and  $2L/D$ . Primary instable state for  $4L/D$  is AC flow regime rather than SP state. Unlike the  $2L/D$  analyses the magnitude of force coefficients for both the upstream and downstream cylinders remain almost same at identical  $\alpha$  values. No sudden change in the force coefficients plots is observed with the transition of flow regime from steady to unsteady state and vice versa. Other than the force coefficient plots, vertical lines representing different flow states at various  $\alpha$  values are also shown in Figure 5-13.

$C_D$  plot shows the attractive nature of both cylinders under counter-rotation with upstream cylinder facing positive drag and downstream cylinder experiencing negative drag. Unsteady flow segments for  $4L/D$  case simulations are shown by  $\sigma$  plots for force coefficients at various  $\alpha$  values in Figure 5-14. Downstream cylinder being less influenced from the upstream flow shows more deviation from the mean force coefficient than the upstream cylinder in both the primary and secondary vortex shedding. In comparison to the  $1.5L/D$  and  $2L/D$  cases the strength of the primary unstable state vortices is more significant in case of  $4L/D$ . As these vortices are of AC flow regime unlikely SP flow regime for lower gap ratio cases.

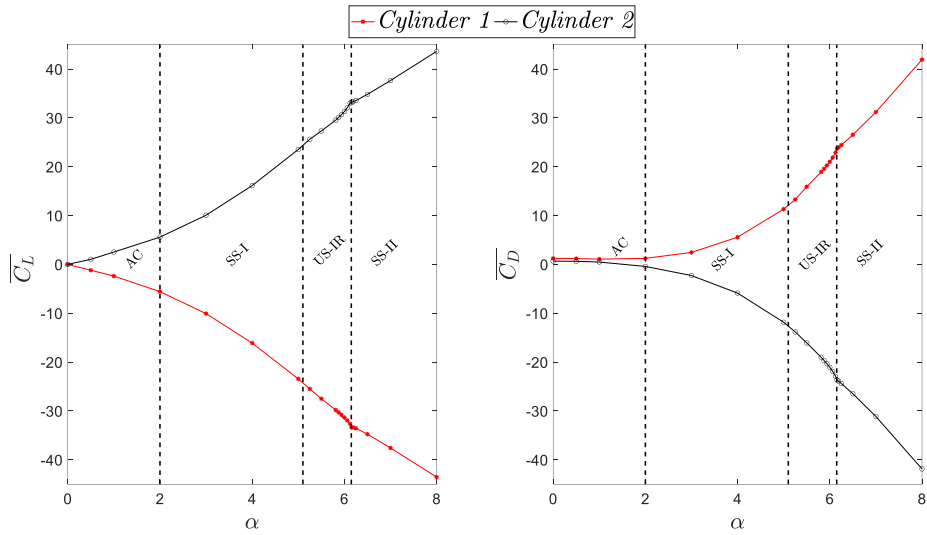


Figure 5-13 Mean force coefficient plots for counter rotating cylinders at 4L/D

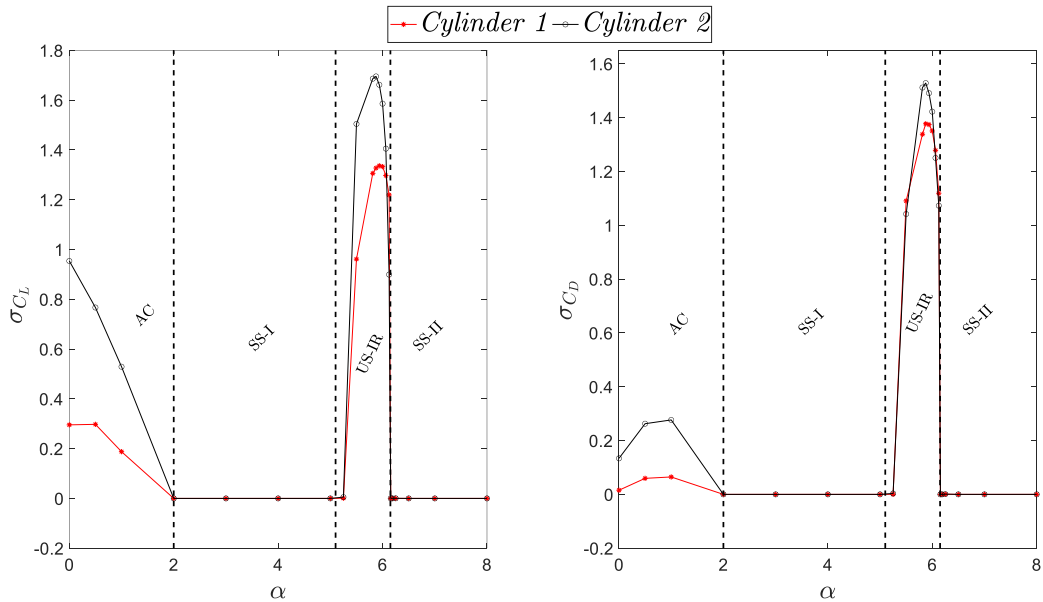


Figure 5-14 Counter rotating cylinders  $\sigma$  contours of force coefficients for 4 L/D at various  $\alpha$

### 5.3 Results regarding Strouhal Number

Strouhal number refers to the non-dimensional frequency by which the vortices in any fluid stream shed. In the present study the St No is calculated by using the prominent frequency of vortex shedding in the whole system of tandem rotating cylinders. Both the cylinder shed vortices with the same frequency and hence the St No for both the cylinders is same. The prominent frequency of the vortex shedding is obtained using the lift coefficient graphs for both upstream and downstream cylinders.

Even in cases where the flow behind the tandem system of circular cylinder seems steady but the Strouhal number still appear in our calculations refer to the fact that there still are small eddies and vortices behind the cylinders, but those vortices are neglected for the sake of reasonable and actual prediction of real flow.

Table 5-2 Strouhal Numbers respective to different gap ratios (L/D), angular rotations  $\alpha$  and Reynolds Number

Strouhal Numbers					
L/D	Alpha $\alpha$	Cylinder	100 Re	200 Re	
1.5	0	UC	0.1329	0.1670	
		DC	0.1329	0.1670	
	1	UC	0.1329	0.1670	
		DC	0.1329	0.1670	
	2	UC	0.0038	0.0076	
		DC	0.0038	0.0076	
	3	UC	0.0038	0.0380	
		DC	0.0038	0.0532	
	4	UC	0.0038	0.0607	
		DC	0.0038	0.0607	
	5	UC	0.0133	0.0076	
		DC	0.0133	0.0076	
	6	UC	0.0076	0.0076	
		DC	0.0076	0.0076	
	2 L/D	0	UC	0.1215	0.1329
			DC	0.1215	0.1329
		1	UC	0.0152	0.1557

Strouhal Numbers					
	2	DC	0.0152	0.1557	
		UC	0.0152	0.0949	
	3	DC	0.0152	0.0949	
		UC	0.0152	0.0645	
	4	DC	0.0304	0.0645	
		UC	0.0304	0.0569	
	5	DC	0.0190	0.0569	
		UC	0.0190	0.0095	
	6	DC	0.0190	0.0095	
		UC	0.0152	0.0038	
	4L/D	0	DC	0.0152	0.0038
			UC	0.1443	0.1689
		1	DC	0.1443	0.1689
			UC	0.1443	0.1708
2		DC	0.1443	0.1708	
		UC	0.1367	0.1557	
3		DC	0.1367	0.1557	
		UC	0.0076	0.0038	
4		DC	0.0076	0.0038	
		UC	0.0076	0.0569	
5		DC	0.0076	0.0266	
		UC	0.0418	0.0076	
6		DC	0.0418	0.0076	
		UC	0.0076	0.0076	

Strouhal Numbers				
		DC	0.0076	0.0076

### 5.3.1 Strouhal Number vs Reynold Number

First comparing the St No considering the change in Reynold Number (100 and 200) we notice that for all the gap ratios, increasing the angular rotation  $\alpha$ , starting from 0 angular rotation till the state where secondary vortices stop shedding, the Strouhal number for higher Reynold number (200) is *more than* the lower Reynold number (100). This flow behavior depicts that *with the increase in flow velocity the vortices from the tandem arrangement of circular cylinders shed with more frequency, reason being the high velocity energetic flow tends to separate from the cylinders surface earlier*. This aspect of vortex shedding is also observed in the simulations for fluid flow of 100 and 200 Reynold number.

### 5.3.2 Strouhal number vs Gap Ratio

At a constant Reynold number, vortex shedding appears in two ranges first the primary one at stationary and low angular rotations and the secondary ones which appear at higher angular rotations. With the increase in gap ratio, considering the overall trend, St No for both the primary and secondary vortex shedding first decrease (moving from 1.5 to 2 L/D) and then increase (from 2 to 4 L/D).

The reason can be that with 1.5 L/D the system was behaving more like a single bluff body but with the increase in gap ratio from 1.5 to 2 L/D shear layer of both cylinders interact with each other more aptly thus decreasing overall vortex shedding rate but with the further increase in the gap ration from 2 to 4 L/D, both the cylinder behave more like separate single cylinders thus the vortices shedding rate increase again.



## CHAPTER 6: CONCLUSION & FUTURE WORK

Inherently, fluid flow surrounding a body has unstable flow behind it, exhibiting various vortical shedding patterns. But flow stabilization can be achieved with the application of rotation to the overall bluff body. Eventually, by carefully regulating the entire rotation of a bluff body, wake behind the bluff body can be controlled resulting in a continuous stable flow. This study focuses on the crucial rotational rates for the start and stop of secondary vortices in an unconfined flow, using two circular cylinders arranged in tandem. A detailed analysis is also conducted on the impact of varying the gap ratios and rotation speeds of the cylinders over the obtained flow regimes and corresponding force coefficients.

In this study, a consistent free stream flow of 100 Reynold number ( $\rho U_{\infty} D/\mu$ ) is applied to two circular cylinders with different gap ratios of 1.5, 2 and 4 L/D (center to center) for each cylinder. Two modes of rotation are observed at each angular rotation ( $\omega D/U_{\infty}$ ). The first mode is when both cylinders are rotated in the same direction (anticlockwise orientation). Secondary when the upstream cylinder is rotated in anticlockwise direction and the downstream cylinder in a clockwise direction. These two sense of rotations capture all the possible combinations of two circular cylinders in tandem arrangement. When applied to cylinders, non-dimensional angular rotations ( $\alpha$ ) range from stationary to the precise  $\alpha$  where the secondary instability disappears.

Based on the vortical shed pattern, several flow regimes and their sub-divisions are described for the co- and counter-rotation of two circular cylinders arranged in tandem. Transitions in flow regimes are observed from 0 to  $6\alpha$  for co-rotation. The 1.5 L/D and 2 L/D gap ratios demonstrate Solitary Periodic (SP) flow, in which vortices shed periodically at low and stationary  $\alpha$  values. Conversely, at stationary and low  $\alpha$  values, alternate co-shedding (AC) flow is observed with a greater gap ratio of 4 L/D, where both cylinders exhibit separate vortical shedding. As  $\alpha$  increases, the flow enters the SS-I flow regime, which is characterized by a steady flow where shear layers continuously shed from the coupled system of cylinders. An additional increase in  $\alpha$  causes the flow to go from the secondary unstable state (SS-I) to the single rotating bluff body (SRB) flow. Two subcategories of SRB flow are identified: integrated SRB flow and segregated SRB flow, which are obtained at low and high gap ratios, respectively. The SS-II flow regime is the result of supplemental  $\alpha$  causing shear layers to wrap around the cylinder with overall steady behavior. It is noted that as the gap ratio increases, the

secondary vortices exhibit delayed beginning and ending as well as delayed transitions between different flow regimes.

Different gap ratios show unique flow regimes for the counter rotation of tandem circular cylinders. At 1.5 L/D, cylinders solely display the SP and SS-I flow regimes. The formation of three separate sub-divisions of the fundamental flow regimes—SP, SS-I, SRB, and SS-II—is depicted by the 2 L/D gap ratio. These sub-divisions are represented as steady state I & II (SS-I & II), secondary unstable - inverted rotation (SU-IR), and secondary unstable (SU-SS-II). when shear layers or vortices are shed differently in the downstream and upstream cylinders. Furthermore, it is seen that these flow regimes switch at significantly higher  $\alpha$  values. In the similar fashion as 1.5 L/D, normal transitions in between the AC, SS-I, SRB, and SS-II flow regimes is demonstrated by the 4 L/D gap ratio. Simulations of different gap ratios for counter-rotating cylinders show that the  $\alpha$  range extends up to  $6.25\alpha$  for the full development of all flow states, with the exception of the 2 L/D case. For a gap ratio of 2 L/D, flow transitions till the atypically higher values of  $12\alpha$  are produced.

The force coefficients grow in magnitude with an increase in applied  $\alpha$  for both the cylinder's co-rotation and counter-rotation. Due to the alteration in location of stagnation points resulting from rotation, tandem cylinders that under co-rotation and counter-rotations exhibit opposing and attracting qualities towards one another respectively. The standard deviation of force coefficient ( $\sigma_{CL}$  and  $\sigma_{CD}$ ) plots, in relation to the mean force coefficient values, is used to trace the presence of the vortex shedding pattern in the specific flow regime. Counter-rotation exhibits a predominant predisposition towards stable flow behavior when compared to the co-rotating cylinder.

Study the impact of high angular rotation in tandem arrangement of circular cylinders at higher flow rates. Tracing of secondary instability for varying gap ratios at higher Reynold numbers.

- Investigation regarding variation of the St No for both the upstream and downstream cylinders in tandem arrangement. Reason and impact of first decrease and then increase of St. No with the increase of gap ratio over increasing rotation rate.
- In detail investigation of the cases where the Strouhal number for upstream and downstream cylinders are different, showing that the vortex shedding of the whole

system of tandem rotating cylinders is with a constant frequency, but the shedding vortex is differently affecting the lift coefficient on upstream and downstream cylinder.

## REFERENCES

- [1] M. M. Zdravkovich, “REVIEW-Review of Flow Interference Between Two Circular Cylinders in Various Arrangements,” *J. Fluids Eng. Trans. ASME*, vol. 99, no. 4, pp. 618–633, 1977, doi: 10.1115/1.3448871.
- [2] J. R. Meneghini, F. Saltara, C. L. R. Siqueira, and J. A. Ferrari Jr, “Numerical simulations of flow interference between two circular cylinders in tandem and side by side arrangements,” *J. Fluids Struct.*, vol. 15, pp. 327–350, 2001, doi: 10.1006/j#s.2000.0343.
- [3] A. Pal Singh Bhinder, S. Sarkar, and A. Dalal, “Flow over and forced convection heat transfer around a semi-circular cylinder at incidence,” *Int. J. Heat Mass Transf.*, vol. 55, no. 19–20, pp. 5171–5184, Sep. 2012, doi: 10.1016/j.ijheatmasstransfer.2012.05.018.
- [4] M. M. Zdravkovich, “The effects of interference between circular cylinders in cross flow††An earlier version as originally presented as an invited paper, entitled ‘Forces on pipe clusters’, at the International Symposium on Separated Flow around Marine Structures, Norwegian Institute of Technology, Trondheim, Norway, 26-28 June 1985.,” *J. Fluids Struct.*, vol. 1, no. 2, pp. 239–261, 1987, doi: 10.1016/S0889-9746(87)90355-0.
- [5] H. M. M. Kiya, M. Arie, H. Tamura, “Vortex shedding from two circular cylinders in a staggered arrangement,” *J. Fluids Eng. Trans. ASME*, vol. 102, pp. 199–204, 1980, doi: 10.1115/fedsm2003-45519.
- [6] M. Kiya, O. Mochizuki, Y. Ido, T. Suzuki, and T. Arai, *Flip-Flopping Flow Around Two Bluff Bodies in Tandem Arrangement*. 1993. doi: 10.1007/978-3-662-00414-2\_3.
- [7] C. H. K. Williamson, “Evolution of a single wake behind a pair of bluff bodies,” *J. Fluid Mech.*, vol. 159, pp. 1–18, 1985, doi: 10.1017/S002211208500307X.
- [8] M. Moriya *et al.*, “Fluctuating Fluid Forces Acting on Two Circular Cylinders in a Tandem Arrangement at a Subcritical Reynolds Number,” *J. Wind Eng. JAWE*, vol. 2001, no. 89, pp. 697–724, 2001, doi: 10.5359/jawe.2001.89\_697.
- [9] S. Mittal, V. Kumar, and A. Raghuvanshi, “Unsteady incompressible flows past two cylinders in tandem and staggered arrangements,” *Int. J. Numer. Methods Fluids*, vol. 25, no. 11, pp. 1315–1344, Dec. 1997, doi: 10.1002/(sici)1097-0363(19971215)25:11<1315::aid-flid617>3.0.co;2-p.
- [10] B. S. Carmo, J. R. Meneghini, and S. J. Sherwin, “Secondary instabilities in the flow around two circular cylinders in tandem,” *J. Fluid Mech.*, vol. 644, pp. 395–431, Feb. 2010, doi: 10.1017/S0022112009992473.
- [11] S. Kumar, B. Gonzalez, and O. Probst, “Flow past two rotating cylinders,” *Phys. Fluids*, vol. 23, no. 1, 2011, doi: 10.1063/1.3528260.
- [12] F. Díaz, J. Gavaldà, J. G. Kawall, J. F. Keffer, and F. Giralt, “Vortex shedding from a

- spinning cylinder,” *Phys. Fluids*, vol. 26, no. 12, pp. 3454–3460, 1983, doi: 10.1063/1.864127.
- [13] D. Stojković, M. Breuer, and F. Durst, “Effect of high rotation rates on the laminar flow around a circular cylinder,” *Phys. Fluids*, vol. 14, no. 9, pp. 3160–3178, 2002, doi: 10.1063/1.1492811.
- [14] S. Mittal and B. Kumar, “Flow past a rotating cylinder,” *J. Fluid Mech.*, vol. 476, pp. 303–334, 2003, doi: 10.1017/S0022112002002938.
- [15] M. R. Rastan, A. Sohankar, and M. M. Alam, “Flow and heat transfer across two inline rotating cylinders: Effects of blockage, gap spacing, Reynolds number, and rotation direction,” *Int. J. Heat Mass Transf.*, vol. 174, p. 121324, 2021, doi: 10.1016/j.ijheatmasstransfer.2021.121324.
- [16] D. Chatterjee, K. Gupta, V. Kumar, and S. A. Varghese, “Rotation induced flow suppression around two tandem circular cylinders at low Reynolds number,” *Fluid Dyn. Res.*, vol. 49, no. 4, p. 45503, 2017, doi: 10.1088/1873-7005/aa6728.
- [17] M. Darvishyadegari and R. Hassanzadeh, “Heat and fluid flow around two co-rotating cylinders in tandem arrangement,” *Int. J. Therm. Sci.*, vol. 135, pp. 206–220, Jan. 2019, doi: 10.1016/j.ijthermalsci.2018.09.014.
- [18] B. G. Dehkordi, H. S. Moghaddam, and H. H. Jafari, “Numerical simulation of flow over two circular cylinders in tandem arrangement,” *J. Hydrodyn.*, vol. 23, no. 1, pp. 114–126, Feb. 2011, doi: 10.1016/S1001-6058(10)60095-9.
- [19] N. Hosseini, M. D. Griffith, and J. S. Leontini, “Flow states and transitions in flow past arrays of tandem cylinders,” *J. Fluid Mech.*, Jul. 2021, doi: 10.1017/jfm.2020.975.
- [20] R. Dubois and T. Andrienne, “Flow around tandem rough cylinders: Effects of spacing and flow regimes,” *J. Fluids Struct.*, vol. 109, 2022, doi: 10.1016/j.jfluidstructs.2021.103465.
- [21] A. R. da Silva and A. M. G. de Lima, “Analysis of flow dynamics around two rotating circular cylinders in tandem and side by side,” *Int. J. Adv. Eng. Res. Sci.*, vol. 7, no. 6, pp. 366–379, 2020, doi: 10.22161/ijaers.76.45.
- [22] M. M. Alam, “Lift forces induced by phase lag between the vortex sheddings from two tandem bluff bodies,” *J. Fluids Struct.*, vol. 65, pp. 217–237, 2016, doi: 10.1016/j.jfluidstructs.2016.05.008.
- [23] M. Ansari, S. T. O. Naeeni, and M. Moradi, “Investigating the Flow and Heat Transfer Characteristics of Two Co/Counter-Rotating Circular Cylinders at a Low Reynolds Number,” *Iran. J. Sci. Technol. - Trans. Mech. Eng.*, vol. 48, no. 1, pp. 193–209, 2024, doi: 10.1007/s40997-023-00657-7.
- [24] H. S. Yoon, J. H. Kim, H. H. Chun, and H. J. Choi, “Laminar flow past two rotating circular cylinders in a side-by-side arrangement,” *Phys. Fluids*, vol. 19, no. 12, pp. 1–5, 2007, doi: 10.1063/1.2786373.
- [25] A. S. Chan, P. A. Dewey, A. Jameson, C. Liang, and A. J. Smits, “Vortex suppression

- and drag reduction in the wake of counter-rotating cylinders,” *J. Fluid Mech.*, vol. 679, pp. 343–382, Jul. 2011, doi: 10.1017/jfm.2011.134.
- [26] A. J. Andre S. Chan, “Suppression of the unsteady vortex wakes of a circular cylinder pair by a doublet-like counter-rotation,” *Int. J. Numer. Methods Fluids*, vol. 65, no. October 2010, pp. 236–253, 2011, doi: 10.1002/fld.
- [27] M. Zhao, “Flow induced vibration of two rigidly coupled circular cylinders in tandem and side-by-side arrangements at a low reynolds number of 150,” *Phys. Fluids*, vol. 25, no. 12, 2013, doi: 10.1063/1.4832956.
- [28] H. Nemati, M. Farhadi, K. Sedighi, M. M. Pirouz, and N. N. Abatari, “Convective heat transfer from two rotating circular cylinders in tandem arrangement by using lattice Boltzmann method,” *Appl. Math. Mech. (English Ed.)*, vol. 33, no. 4, pp. 427–444, 2012, doi: 10.1007/s10483-012-1561-6.
- [29] N. Mahír and Z. Altaç, “Numerical investigation of convective heat transfer in unsteady flow past two cylinders in tandem arrangements,” *Int. J. Heat Fluid Flow*, vol. 29, no. 5, pp. 1309–1318, 2008, doi: 10.1016/j.ijheatfluidflow.2008.05.001.